Design, Implementation and Evaluation of Cooperative Methods for Short-Term Compensation of Deviations from the Load Schedule for Dual Demand Side Management

by

Mehrdad Biglarbegian

School of Industrial Engineering

Department of Energy

Supervisor:

Dr. Fabio Rinaldi

There are no incurable diseases, only the lack of will and

There are no worthless herbs, only the lack of knowledge

Avicenna, Iranian Polymath

Abstract

The transition of conventional power system into the flexible smart grids is underway. The future increase of decentralized energy conversion by interaction of thermal and electrical generations as well as changes the basic conditions introduce new opportunities and challenges. One of distributed controlling methods is a concept of a rational agent. An agent can apprehend any changes through actuators or the environment. The household submits the consumptions for the agent operator and aggregator negotiates with each household on schedules for the next day. The aggregator negotiates with each household on a load schedule, which will be followed the next day, based on forecasts for demand, generation, and weather. In the second phase, a short-term balancing mechanism monitors the system and detects possible deviations due to weather changes or unexpected user behavior. However, for the short term balancing investigation and comparison of several options is planned.

One of the options is to reduce the consumption or switching to the alternative schedule. The second option is to analyze the new states of a system in presence of the deviations. By proposing the alternative solutions, try to stick to the current schedule as much as possible. This approach works on the short-term time intervals for the investigations and imposing the new strategies.

The potential of Photovoltaic as an electrical generator, micro-CHP to heat and power generation and heat pump as a representative of thermostatically controlled loads are used. In the photovoltaic, the Kalman filter method is used to estimate the generation at the current time interval. The algorithm for calculating the micro-CHP operation and the dynamic behavior of the heat pumps are studied. In addition, the methodology for the optimum dispatching the excess of generations among the deviated loads is presented.

Acknowledgments

This thesis is the results of the research in ACS located at E. ON Research Center Institute of RWTH Aachen with joint project with Politecnico di Milano. First, I would like to express the greatest gratitude to Professor Antonello Monti for trusting me and giving the opportunity to work under his guidance at E. ON research center. I would like to acknowledge to my supervisor, Doctor Fabio Rinaldi for his guidance and successive support throughout my graduate studies at Politecnico di Milano. Moreover, I would especially like to thank Professor Delfanti, for serving on my examination committee and providing additinal insight through the impressive course "Smart Grids and Regulation for RES."

Many thanks go to my colleague Ivelina Stoyanova for her suggestions and comments during collaborating in ACS group. Ivelina, your knowledge and continuous presence helped me a lot in this research and I can't forget your dominant role and confiding in me during this period.

In my daily life, I have been blessed with so many wonderful friends that I'm afraid I cannot mention them one by one here. I would like to sincerely thank my friends, Behzad, Hassan, Mojtaba, Amir, and Leandro for unforgettable memories.

At this point, I am truly interested and proud to say the deepest thankful to my family members. From bottom of my heart, the greatest appreciation goes to my dear father and my nice mother for their emotional asserting and advising permanently. Mohammad and Behzad, I have been blessed to have brothers like you due to unlimited kindness supporting in all of the aspects particularly for my master thesis. Thanks for your continuous encouragement and availability emotionally and scientifically. I greatly appreciate my clever grandmother, calm uncle Masoud, unique uncle Mehdi, fantastic sister in law, Zahra, cute nephew, Alee, and my new and warm relatives, Rezvani's families. Furthermore, thanks should be also extended to Arshad, Sabina, Bijan and Dana for helping me and any sort of distraction in Germany.

Last and not least, I would like to express the thankfulness to my fiancé, Fatemeh for her boundless encouragement and beautiful relation. None of this would have been possible without your supreme patience, great inspiration, love, and understanding. I warmly appreciated your concerns, kindhearted endeavors, and everlasting motivations by this long distance.

Declaration

I declare that this thesis does not incorporate without acknowledgment of any material previously submitted for a degree or diploma in any university, and that to the best of knowledge it does not contain any materials previously published or written by another person except where due reference is made in the text.

Mehrdad Biglarbegian

List of Figures

List of Tables

Nomenclatures

Symbols, parameters, and variables:

a	Ideality Factor Parameter of the PV Model	eV
a_0	Error Model for the PV Estimation	
a_k	Parameter Estimation for PV at Time Step of k	
C	Specific Heat of the Water	$4.18\,{}^{\mathrm{kJ}}/_{\mathrm{kg.K}}$
d_m^n	Distance Between the Demands and DER	m
E_g	Energy Band Gap	eV
$e_{\min}$	Threshold Value for Electricity Production of CHP	kW
e_d	Electrical Demand	kW
$e_{production}$	Excess Electrical Production by CHP	kW
e_{in}	Electrical Power Import from the Grid	kW
e_{out}	Electrical Power Export from the CHP to the Grid	kW
G	Total Radiation on Surface	${}^{\mathrm{W}}/_{\mathrm{m}^2}$
G_{ref}	Irradiance at SRC[1]	$1000\,{}^{\mathrm{W}}/_{\mathrm{m}^2}$
h_d	Thermal Demand	kW
$h_{storage}$	Heat Storage Energy Level	kWh
h_{CHP}	Thermal Capacity of the CHP	kWh
$h_{high,CHP}$	High Heat Storage Energy	kW
$h_{low,CHP}$	Low Heat Storage Energy	kW
$h_{s,a}$	Average Heat Storage Energy Level	kWh
h_{aux}	Axillary Burner Capacity	kW
$h_{aux,\max}$	Maximum Axillary Burner Capacity	kW
$h_{aux,\min}$	Minimum Axillary Burner Capacity	kW
$h_{primary}$	Thermal Capacity of Prime Mover	kW
$h_{primary,\max}$	Maximum Thermal Capacity of Prime Mover	kW
$h_{primary,\min}$	Minimum Thermal Capacity of Prime Mover	kW

[1] Standard Rating Condition

I_{ph}	Internal Equivalent Current Source of PV	A
I_{sr}	Short Circuit Current of PV	A
I_s	Reverse Saturation Current for the PV Model	A
I_{sr}	Reference Reverse Saturation Current of the PV Model	A
I_{PV}	Output Current of PV for the PV Model	A
k	Boltzmann's Constant	1.38066×10^{-23} J/K
K	Temperature Coefficient for the PV Model	$1/\mathrm{K}$
K_t	Kalman Filter Gain for the PV Estimation	
m	Mass Flow Rate in the Storage Tank	kg
$\hat{P}_{\max\_PV}$	Maximum Output Power of PV	kW
$P_n^{\max}$	Maximum Power Capacity of DER	kW
ΔP_m	Deviated Real Power from the Assigned Schedule	kW
P_k	State Variance Matrix	
q	Electron Charge	1.62×10^{-19} Coulomb
Q_k	Process Variance Noise for the PV Estimation	
R_s	Series Resistance of the PV Model	Ω
R_{sh}	Shunt Resistance of the PV Model	Ω
R_k	Measurement Error for the PV Measurement	
S_m	Complex Demand Power	kW
S_n	Complex Generated Power of DES	kW
t_r	Minimum Run-time for Starting-Up the CHP	15 minutes
ΔT	Temperature Difference	°C
T	Temperature	°C
T_{ref}	Reference Temperature	°C
$T_{high,CHP}$	High Heat Storage Temperature in CHP	°C
$T_{low,CHP}$	Low Heat Storage Temperature in CHP	°C
V_t	Thermal Voltage of Array in Diode Model	26mV
V_{PV}	Output Voltage of PV	V
v_k	Measurement Noise	
w_k	Process Noise	
$\hat{x}_k$	State Space Vector of the PV Estimation	
y_k	Generated Power at Time Step of k	

z_k	Measurement Output of PV	
η_k	Efficiency of PV at Time Step of k	
η_0	Reference Efficiency of PV at 25 °C	
ξ	Coefficient of Cell Temperature	$1/K$
$\eta_{thermal}$	Thermal Conversion of the CHP	
η_e	Electrical Conversion of the CHP	

Abbreviations

2DSM	Dual Demand Side Management
CHP	Micro Combined Heat and Power
COP	Coefficient Of Performance
DAM	Day Ahead Market
DER	Distributed Energy Resources
DG	Distributed Generation
DR	Demand Response
DHW	Domestic Hot Water
DSM	Demand Side Management
HEM	Home Energy Management
HP	Heat Pump
ICE	Internal Combustion Engines
KF	Kalman Filter
GT	Micro Gas Turbine
MAS	Multi Agent System
PEM	Proton Exchange Membrane
PV	Photovoltaics
RES	Renewable Energy Sources
SM	Stirling Motor
SOFC	Solid Oxide Fuel Cell
TCL	Thermostatically Controlled Load
VPP	Virtual Power Plants

Table of Contents

1. Introduction

1.1. Future of Smart Grid

Over the last years, the energy problem have become of the important challenge in all over the world. Limited number of the power plants, trying to keep the demand and supply balanced at all times as long as environment issues for reducing the emissions are substantial concerns in the future energy. A significant proportion of energy is consumed to meet the building energy demand, especially those associated with the residential application [1]. Increasing the energy efficiency, minimization of overall energy consumptions, increasing the reliability of the power system network are the long-term approaches for to prevailing these challenges. Many sustainable energy technologies are under development especially for electric production in medium and low voltage levels. The energy storage system, micro grids, Distributed Generation (DG) will convey the future of the smart grid.

The energy storage system is usually used for meeting the peak demands; improve the power quality and reducing the operational cost. Although, the higher installation cost of the storage system and lack of standards are the most important challenges in this field, these technologies will be utilized in the next five years [2]. On the other hand, micro grids tries to meet the local demand to ensure the grid reliability, easier energy management will be highly used over the next years in military utilities, hospitals and so on.

DG refers to small-scale energy generation system in distributed level. Photovoltaic (PV) systems, Wind Turbine (WT), Micro Gas Turbine (GT), Micro Combined Heat and Power (CHP), Fuel Cells (FC) are the most well-known DGs in the distributed system. Whenever the DG units use the renewable energy as primary, which called Renewable Energy Source (RES) have significant environmental benefits due to lower emissions. In addition, lower losses, enhancing the power reliability and reducing the investment risk compare to transmission lines are the other benefits of using the DGs in power system network. Currently, the penetration of

DG components in medium and low voltages is increasing all over the world although the uncertainty and unpredictability is inevitable especially in PV system [3].

If several DGs connect together to operate as a single unit for energy production the concept is called Virtual Power Plant (VPP). The future of smart grids and VPP is contributed to electrical and thermal generation of DG units as shown in Figure 1.

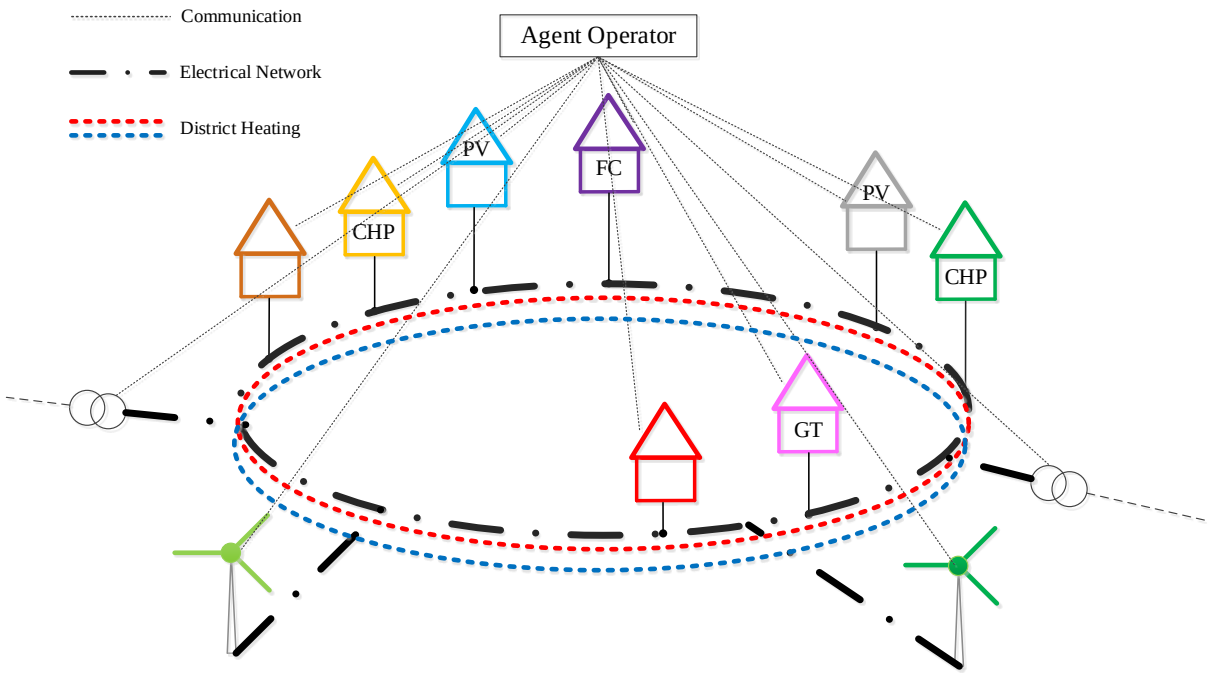

Figure 1: VPP in future smart grids

The needs for strong communication infrastructure (mainly wireless technologies) create new potentials for increasing the adoption of these technologies. It is expected that the future of smart grid mainly will discuss emergence of DG systems, Demand Response (DR) actions, market innovation, and digital energy systems.

1.2. Dual Demand Side Management

Demand Side Management (DSM) was widely discussed in the 1980's as the alternative to supply side "overspending" in energy systems [4]. The final goal of DSM is to make a balance between the load consumptions and the generations in the power system. However, planning, implementation, monitoring of distribution network to influence the customer consumptions will produce desirable and more flexible changes in load shape patterns:

The generators in the power systems are the large power plants and RES. Due to the limited capacity, technical issues of the transmission lines, the power plants are restricted to produce higher energy. On one hand, the unpredictability of volatile RES that changing the over the time and on the other hand, the nonlinear behavior of the end users, balancing is a constant challenge for the network operators. The focus of DSM studies is dedicated on the final user in residential, commercial, and industrial utilities as the most important players in the network. The industrial loads due to relatively constant energy consumption over the working hours are exempted from DSM studies. In addition, compensating the fluctuations at medium and high voltage level would result in a high cost solution and large investment. Usually, controlling the loads and power injection of DER are cheaper than establishing the new power plants or costly battery storage system. Most of the studies allocated by commercial and residential loads in low voltage electrical networks [5], [6]. The main important aims of DSM approach is to

1. Reduce the peak loads
2. Increase the demand during off-peak loads
3. Shift the load from on-peak to off-peak
4. Reducing energy consumptions
5. Making the load flexible

In centralized controlling approach for conventional power system, non-dynamic DSM strategies utilized for increasing the efficiency of the system. Higher efficiency can be obtained by using dynamic strategies for exploitation of RES and infrastructure of DG in the power system. The dynamic DSM, does not necessarily reduce the energy consumption. The concept of DSM usually affect only on the consumption pattern. If a process is interrupted for some reasons, it migh catch up again and rebound effect takes place. This needs effective strategies in DR sections for improving the process quality [7]. Furthermore, DSM policies are classified in four differnt classes [6], [8]:

1. Energy Efficiency
2. Time of Use
3. Demand Response
4. Spinning Reverse

The lower edge and the most important part of DSM is Energy Efficiency. All of the actions for improvement the physical properties of the system belongs to this class. For example, exchanging an inefficient device with a better one is the one of the common strategies in this level. Time of Use mainly allocated to market challenges for improvement the consumers' behaviors with dynamic and non-dynamic tariffs [8]. As we mentioned above, DSM policies try to stick to the end-user efficiencies. However, for better utilization of the power system network, the more active and productive strategies are needed. Demand Response (DR) is the one of the most important levels in DSM policies. Demand Response (DR), refers to all of the infrastructures of the communication system between the network operators and the final end users. Reflecting grid congestions, excess of RES and limitation for stabilizing user behaviors are the main important actions of this class.

Two are the most common strategies are Direct Load Control (DLC) and Price-Based Control (PBC). DLC strategies provide the flexibility to switch off one or multiple devices within the customer households. Sending a signal for open a circuit as an interruption the electricity consumption is easy imagination of this strategy. The concept of PBC is used for influencing the demands side using the time variation in electricity price.

Spinning Reveres is defined for all of the activities for generation capacities to respond the system within seconds for compensation of generation to meet the demand needs.

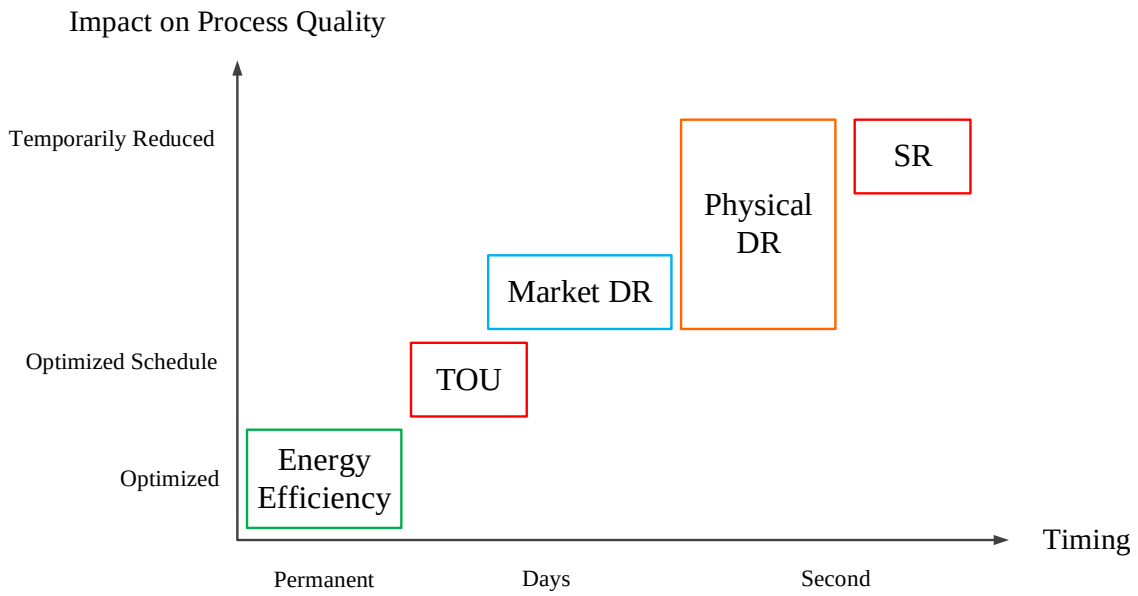

Figure 2: Categories of DSM

In distribution system, thermal energy accounts for a relatively high fraction of the end-user consumptions. For increasing the DSM potential, the interaction of thermal and electrical demand should be considered. To fully exploitation of the potential of dynamic DSM, the interplay of thermal and electrical demand has to be considered. The concept of 2DSM for expansion the DSM vision, helps to increase energy efficiency and flexibilities in generations/consumptions by using the potential of thermal storage in order to support the integration of RES. The energy efficieny of the cities can be increased by alternative heating systems like CHPs, FCs, or heat pumps. These alternatives link the electrical and thermal grids directly. Larger time constants of thermal systems respect to electrical systems opens wider range of flexibility for supporting RES and applying DR strategies more effectively [9].

1.3. Load Balancing Concept

Load balancing is an essential process in distribution system level. The load balancing helps the network operator to enhance the network performances. Due to highly exploitation of RES and stochastic end-user power consumption, usually it is very difficult to fulfill SDM actions all over the time.

Load balancing algorithms are categorized in two different stages: static and dynamic. The static load balancing algorithms are suitable for stable environments. The convergence of static algorithms is not flexible with dynamic changes of the states. In contrary, the flexibility of the dynamic algorithms creates adaptable results with real-time changes. Memory storage for replication, computation complexity of the algorithm are the most common challenges in different algorithm methods [10], [11].

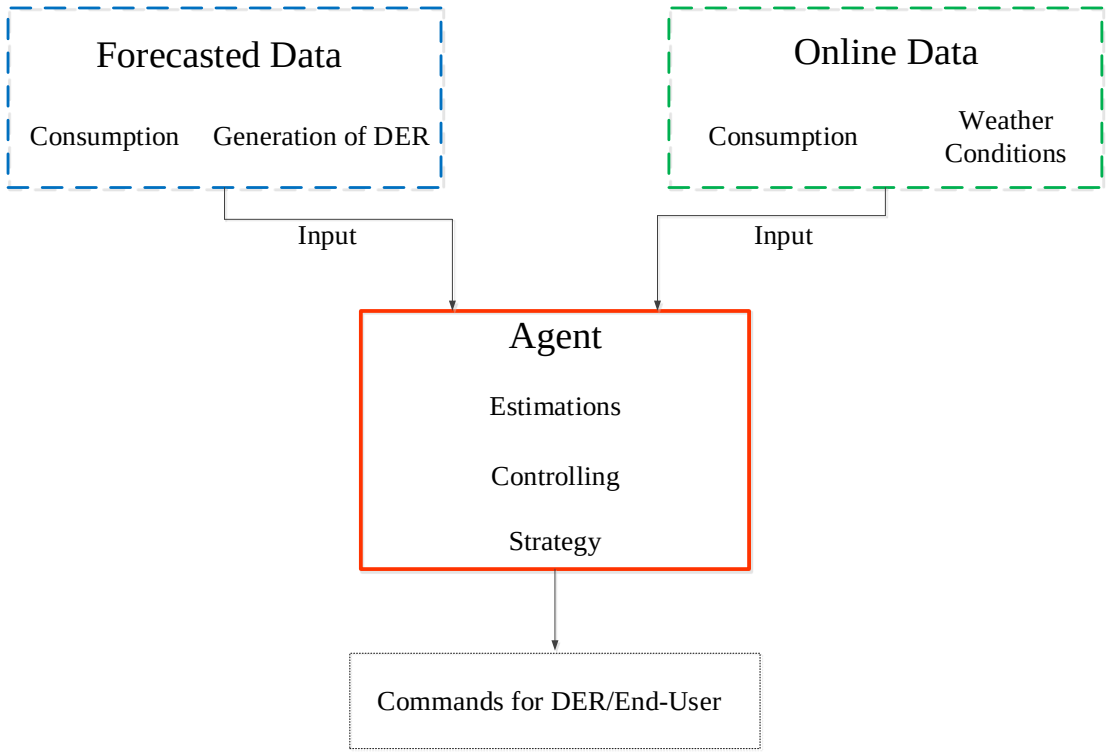

Figure 3: Input/Output data of the compensation

The agent receive the forecasted data and online data. The forecast data, which composed by consumption and the generation of DER is considered as a base schedule. It means the network operator tries to follow the schedule as close as possible. The online data shows the current consumption power of the end-users and weather conditions. Figure 3 shows the interaction between the input and output data of agent structure for the compensations. First, the agent ties to estimate the current situation of the DER. The agent based on predefined model of the DER or the estimation methodology. Next, the agent compares the forecasted consumptions and the current one; on the other hand, make a comparison between the forecasted generations and the current generations. If the deviation is discovered, the agent based on the own strategy tries to control and compensate the deviations as shown in Figure 4.

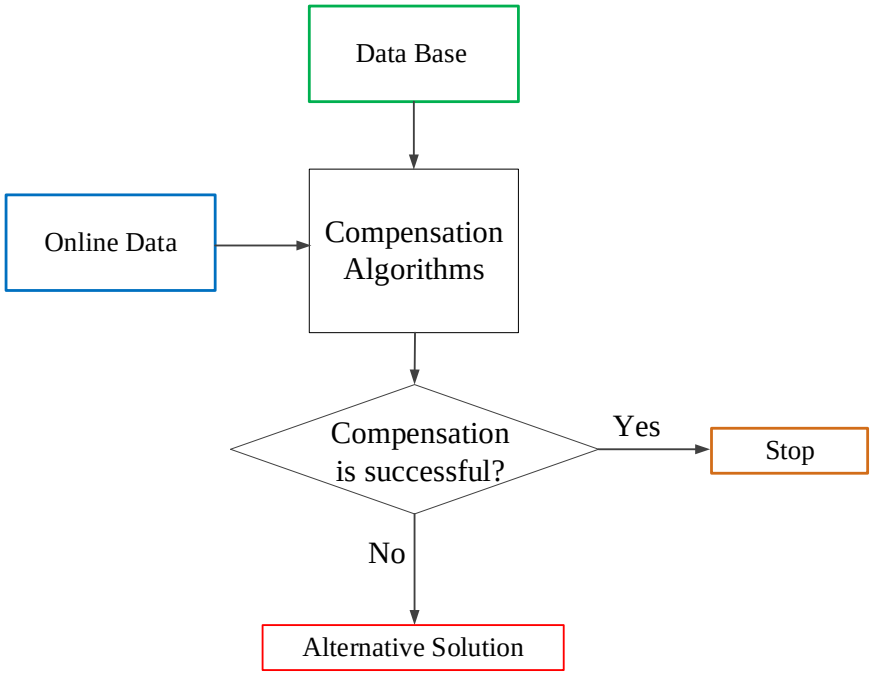

Figure 4: General algorithm for compensation of the deviations

1.4. Thesis Framework

The goal of this thesis is to compensate of the deviated loads by fully exploitation of RES. At first, the modeling of steady state and dynamic behaviors of PV, HP and CHP in short time intervals. For the modeling and estimation of the PV Kalman Filter (KF) algorithm is proposed. Secondly, the dynamic behavior of the HP as a representative of TCLs is studied.

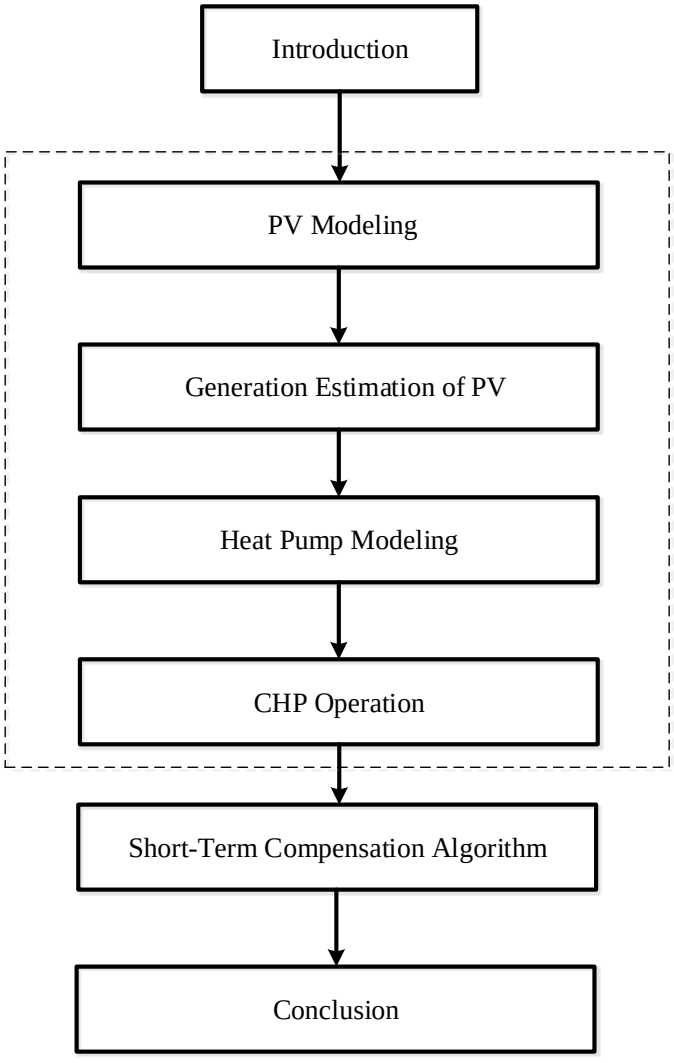

Figure 5: Thesis framework

Also in this work, agent-based modeling for individual methodology actions is used. It is assumed that each agent is a system component with a certain level of autonomy. The agents can also communicate with other agents locally in special patterns. A large number of the agents communicate self-oriented or team-oriented to achieve Multi-Agent System (MAS) objectives.

The agents in an aggregated way can share their requested active/reactive power data among the agents' participants.

In the other words, a specific agent has access to the load profiles of consumers and the generations of RES in its region individually. The agent according its own strategies or algorithms, analyze the environment to make an independent decision. The agents use the strategies to track the assigned schedule and make compensations for following the stable plans in case of deviations. The further decisions are transmitted to the end-users or DGs by contributing the technical factors. The agents have the ability to add, remove, control, or implement a specific algorithm for the production units or the consumer behaviors. The agents interact cooperatively in their defined zones without any communication constraints.

In this work, only technical issues and limitations for the load balancing procedures in decentralized approach is considered. Thus, energy flat-rate tariffs, any financial constraints, or priorities for the unscheduled switching devices are neglected.

2. Modeling of System Components

2.1. Introduction

Generation from RES generally does not match end-user load profiles. Furthermore, the time variability of RES can cause the lack or surplus of energy in the grid [12]. Therefore, the coordination and integration of RES is a central task for the development of future grids. In order to use better the network capacity and to enable load balancing procedures in short-term range, reliable models of active components in the grid and effective estimation of their behavior are necessary. In this chapter, the models of the active components are presented as a primary tool for accurate estimations.

In this work, the research of RES is focused on the impact of PV, HP, and CHP on the distribution grid. Innovations in the development of PV technologies increase the importance of research of suitable modeling and control techniques. PV is one of the most attractive alternative energy source for power generation, especially as installation in residential areas at low voltage level [13], [14].

On the other hand, popularity of HP is growing rapidly due to its high efficiency, quick start-up, and the possible utilization for both heating and cooling. The number of installed HP in residential applications is expected to increase further in future [15], [16].

According to forecasts, fifty percent of all households will install CHP in the next two decades. The most advantages of CHPs are the flexibility to generate electrical and thermal energy simultaneously, and the higher efficiency with respect to conventional power plants [17], [18].

In this chapter, first the model of power generation by PV cells is studied. The model is helpful to find the actual output power of the PV for more precise estimations. Secondly, an aggregated model of the dynamic behavior of HP is studied, as a representative of Thermostatically Controlled Loads (TCL) in residential applications, including a model of the dynamic behavior of the end-user. Finally, an algorithm and operation of CHP in a single house is explained.

2.2. Photovoltaics Modeling

According to the policies and statistics, solar, wind, biomass and geothermal become a larger part of the fuel mix until 2040 [19]. Especially PV is expected to be highly exploited in the future due to its potential for decreasing global warming.

PV cells absorb the beam radiation from the sun and convert them to electrical energy. The amount of generated energy by PV directly depends on the beam radiation and the temperature of the environment [13]. If the irradiation is high, generated current of each PV cell is high, which results in higher output power. However, various weather conditions can substantially affect the efficiency of the PV output power. High ambient temperature above the reference temperature of 25°C cause current saturation current of the PV decreases the generated power and its efficiency.

Previous studies show that power generation of a PV is stochastic because of fluctuations [20], [13]. The fluctuations strongly depend on weather conditions like temperature, cloudiness, and humidity. Therefore, in order to obtain reliable results for the planning of reasonable actions by the agent, reliable estimation of the PV output is necessary. Estimation is useful by agents, retailers, and companies for more precise short- and medium-term planning.

A PV model is presented in Figure 6. The current source represents an ideal model of a PV. Except for the internal resistance of a PV and small current leakage, the losses of PV are negligible [21].

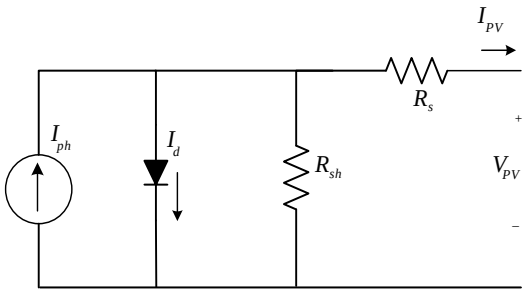

Figure 6: Equivalent circuit of PV

In Figure 6, I_{ph} defines the internal equivalent current source. This current is directly proportional to the irradiation of the sun's beams. Its magnitude is affected by the PV temperature [14]. In the model adopted from [13], R_s represents a series resistance of the internal losses, R_{sh} is the parallel resistance of the diode, and V_{PV} indicates the output voltage. The ambient temperature has some impact on the generated power of the PV. According to [13], ambient temperature above the reference temperature reduces the output current of the PV as following:

$$I_{ph} = (I_{scr} + K\Delta T)\frac{G}{G_{ref}} \tag{1}$$

In equation (1), G_{ref} is the reference sun irradiation of $1000\ W/m^2$ based on [21]. G is the actual sun irradiation and K is the temperature coefficient in $mA/°C$, which affects the saturation current. Further, I_{scr} is the short circuit current of the PV cell at the temperature reference (25°C).

The actual reverse saturation current is introduced below, corresponding to the changes in ambient temperature:

$$I_s = I_{sr}(\frac{T}{T_{ref}})^3 \exp[\frac{qE_g}{ak}(\frac{1}{T_{ref}} - \frac{1}{T})] \tag{2}$$

In equation (2), T represents the ambient temperature in Kelvin and T_{ref} is the reference temperature of 25°C.

The output current of the PV and the maximum output voltage of the PV are calculated according to (3) and (4), respectively. V_t is the thermal voltage of diode is assumed to be 26mV.

$$I_{ph} = I_{ph} - I_s[\exp(\frac{V_{PV} + R_s I_{PV}}{V_t a}) - 1] - \frac{V_{PV} + R_s I_{PV}}{R_{sh}} \tag{3}$$

$$\hat{P}_{\max\_PV} = I_{PV} \times V_{PV} \tag{4}$$

The maximum output power is relevant for the maximization of the exploitation of the PV. Thus, three analysis scenarios are defined in comparison with results of previous studies on [1], [8] by manipulating the equation (4). The obtained results confirm the mentioned

references. Appendix A contains the validated results of the PV modeling which depict these scenarios.

Figure 7 shows the schematic of the analytical output power of the PV considering the environmental data. In this study, the losses of the power electronic devices or any other electrical components are neglected.

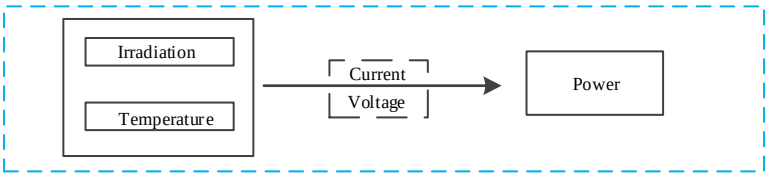

Figure 7: General configuration for obtaining analytical output power

The parameters presented with semi-empirical equations in this section are used to calculate analytically an initial voltage-current curve. In the next step, the PV model is used in the estimation to calculate the output power more precisely. As mentioned before, the model strongly depends on weather conditions such as temperature and cloudiness. To convey the data estimation more accurately, it became necessary to improve the analysis of the weather forecast. The estimation of the PV model needs the analytical output power for establishing the state space matrix that is fully described in the next section.

2.3. Output Power Estimations of the PV

As mentioned before, due to the nonlinear characteristics of the PV, usually it is very difficult to predict PV generation. In the previous section, a simple model is proposed based on semi-empirical relations of the PV generation. Although the model has been developed to calculate the energy generation, more effective forecast method of the PV is required. Therefore, estimation is used for precise short-term prediction of the PV generation.

The proposed method employs linear regression model by prediction of KF method to estimate the system states more precisely against initial errors, noises and disturbances [22]. The objective is to predict the PV power generation for the next time interval according to the generated power in the last three intervals.

The estimation has two steps:

1. Data processing
2. Estimation of the unknown mathematical parameters

In the first step, data processing, we consider the characteristics of the PV generation according to weather conditions. As mentioned in section 2.2, the PV output power is directly affected by ambient conditions. Due to the variable weather conditions, the descriptive data processing are categorized in three terms [23]:

1. Good
2. Variable Cloudy
3. Bad

This categorization allows to analyzing and comparing the quality of estimation based on a reference index [23]. The reference index is assumed 8. The category “Good” is indicated by index 0 or 1, which refers to a sunny day with continuous coverage, while the category “Bad” is indexed with 7 or 8. The category “Variable Cloudy” is defined with index 3 to 6. In this

work, we only consider Good and Variable Cloudy classes. Figure 8 illustrates the output power of Good and Variable Cloudy classes.

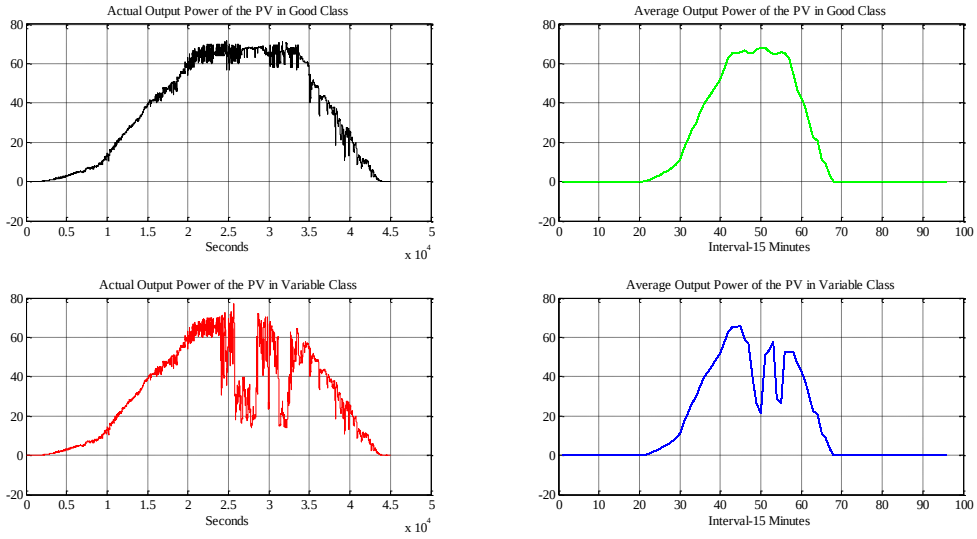

Figure 8: Output power of the PV in good and variable classes for the research

2.3.1. Estimation of the Unknown Parameters

For the estimation of the parameters, the current efficiency in employed in regression model and calculated based on the weather forecast [22]:

$$\eta_k = \eta_0(1-\xi(T_{ref} - T_k)) \tag{5}$$

where ξ represents the cell temperature coefficient and η_0 is the efficiency at the reference temperature of 25°C. For operation below 25°C, the PV efficiency is calculated with the reference temperature. In the next step, the output power is categorized with the regression model:

$$y_k = a_0 + \sum_{i=1}^{p} a_{k-i} \times y_{k-i} \frac{\eta_k}{\eta_{k-i}} + v_k \tag{6}$$

In equation (6), y_k is the estimated value for the PV power output for the next time interval, based on previous measurement data y_{k-1}. a_0 represents an error model, which is assumed as one; η_k and η_{k-i} describe the efficiency at the time interval k and $k-i$, respectively. In this model, $p = 3$; this means, for the calculation of the current value for the PV power output, the last three values are considered. A dynamic process of the PV generation is presented by following equations:

$$x_{k+1} = A_k x_k + w_k \tag{7}$$

$$z_k = C_k x_k + v_k \tag{8}$$

$$A_k = \begin{bmatrix} 1 & 0 & 0 & 0 \\ 0 & \frac{\eta_k}{\eta_{k-1}} & 0 & 0 \\ 0 & 0 & \frac{\eta_k}{\eta_{k-2}} & 0 \\ 0 & 0 & 0 & \frac{\eta_k}{\eta_{k-3}} \end{bmatrix} \tag{9}$$

$$x_k = \begin{bmatrix} a_0 \\ a_{k-1} \\ a_{k-2} \\ a_{k-3} \end{bmatrix}^T \tag{10}$$

$$C_k = \begin{bmatrix} 1 & y_{k-1} & y_{k-2} & y_{k-3} \end{bmatrix} \tag{11}$$

In (7) to (11) the measurement noise v_k and process noise w_k are assumed to be normally distributed with zero mean value. In the model, z_k is a scalar product and defines the output power of the PV. Matrix A_k is the efficiency matrix and composed using η_k. In equation (10), x_k is a vector of unknown-parameters that illustrates the system states to estimation process shown in Figure 9.

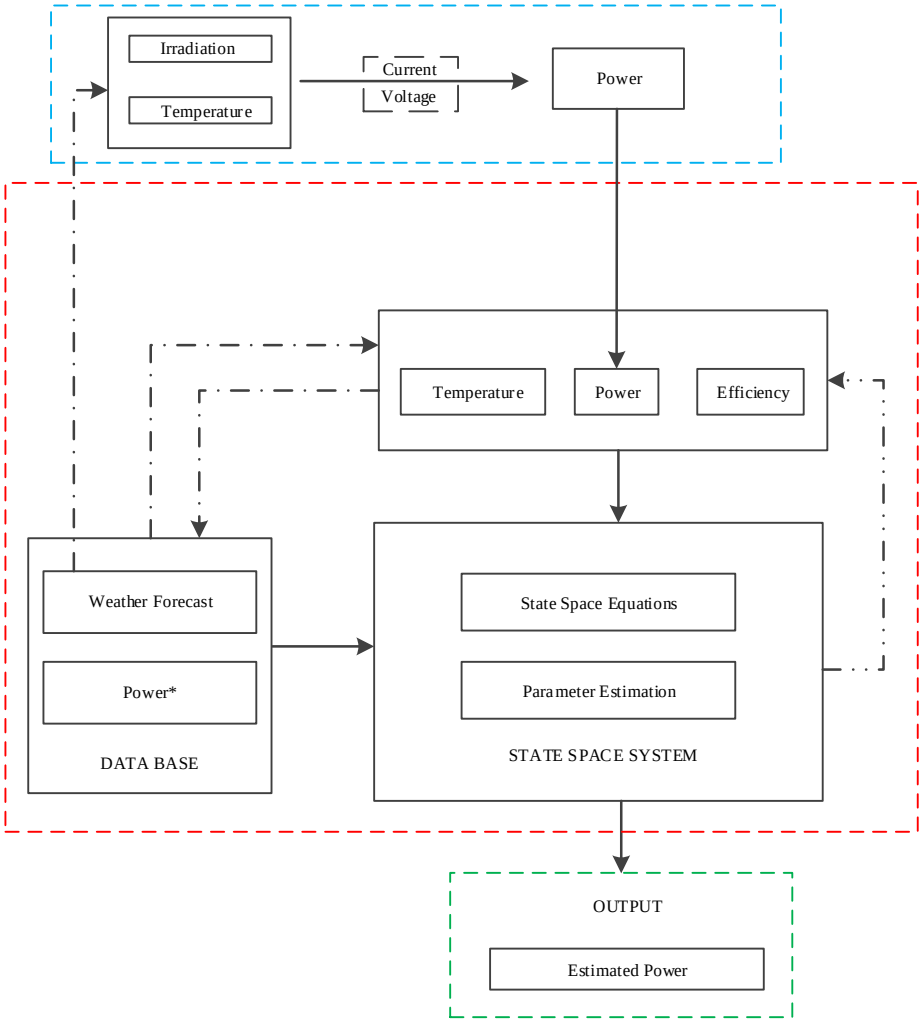

Figure 9: PV estimation model

Data processing is highlighted with the blue dashed line. Based on the technical parameters and data from the environment, the PV output power can be calculated. This part is fully described

in section 2.2-Photovoltaics Modeling. The middle part of figure, marked with red dashed line, refers to unknown parameter estimation by KF algorithm. The estimation algorithm is introduced in the next section.

2.3.2. Kalman Filter Algorithm

The KF method is a nonlinear estimation algorithm based on series of measurements over time and recursively calculating the unknown variables. Provided the state space equations of the system are unknown, the KF algorithm is applicable for any physical system with limited measurements [24]. The result is obtained through prediction and updating the unknown variables. Figure 10 shows how the parameters for implementing the KF.

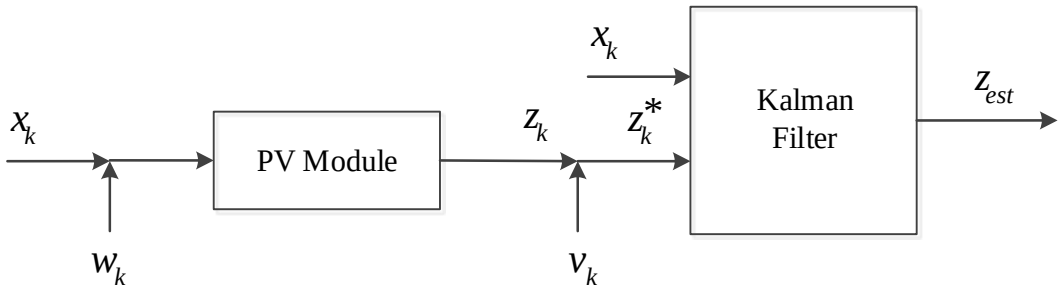

Figure 10: KF input and output schematics

The estimation should be repeatedly calculated via filtering algorithm. If the parameters converge to the constant, the prediction is considered successful.

$$\hat{x}_{k+1|k} = A_{k+1}\hat{x}_{k|k} + v_{k+1} \tag{12}$$

$$P_{k+1|k} = A_{k+1}P_{k|k}A_{k+1}{}^{T} + Q_{k+1} \tag{13}$$

As shown in equation (12), $\hat{x}_k$ is the estimation state vector that shows the state transition in the model. Propagator matrix A_k allows forecasting the state in the time $k+1$. If the covariance matrix of the state estimation at time k is called P_k, then covariance matrix of $\hat{x}_{k+1}$ is defined by equation (13), where Q_k is the normalized covariance matrix of the noise v_k [24]. The measurement is linearly connected to the state transitions as following:

$$z_k = C_k \hat{x}_k + R_k \tag{14}$$

In equation (14), R_k is the normalized covariance matrix of the measurement error. The KF should update the state transition according to equation (15):

$$\hat{x}_{k|k} = \hat{x}_{k|k-1} + K_k (z_k - C_k \hat{x}_{k|k-1}) \tag{15}$$

Where K_k represents the KF gain and is defined by (16):

$$K_k = P_{k|k-1} C_k^{\ T} (C_k P_{k|k-1} C_k^{\ T} + R_k)^{-1} \tag{16}$$

Finally, the covariance is updated through (17):

$$P_{k|k} = (1 - K_k C_k) P_{k|k-1} \tag{17}$$

By repeating from the equation (5) to (10) and applying the KF algorithm from equation (12) to (17), and the short-term estimation of the PV generation is implemented. Appendix B shows a simple testing scenario of the estimation of the PV generation.

3. Thermostatically Controlled Loads

3.1. Introduction

Recent studies for European countries show that the energy consumptions of residential applications is increasing and the demand of the industrial loads is decreasing. This effect has increased further after financial crises[2], as companies in developed countries outsource factories to developing countries [25]. At the moment, buildings account for 40% of total amount of energy in Europe and most of the energy consumptions in urban areas pertain to thermal devices [15]. Therefore, DR strategies include approaches for the control of TCLs. Accordingly, energy efficiency of the devices and studies on the usage of TCLs have been central research topics in recent years [26], [27].

The research of the dynamic behavior of TCLs primarily considers refrigerators, electric water heaters, air conditioners, Heating, Ventilation and Air Conditioning (HVAC) and HPs [28]. These devices, due to the thermal storing capacity, are suitable candidates for load balancing strategies in smart grids. In general, non-thermostatically controlled loads[3] are classified as online demand; it means the operators should provide the requested power immediately through the network. TCLs create flexibilities due their potential to store thermal energy. These flexibilities can be used by the grid operator to apply compensation load balancing procedures, or to switch to a more adequate control strategy according to the current power demand.

HPs play a major role in the future of the grids due to their high efficiency [15]. Their performances and characteristics were object of numerous articles over the last years, improving the model accuracy. Transfer functions are derived by identification techniques for obtaining linear TCL models in several articles [29], [30].

There are different approaches for the modeling of residential HPs, such as calculation methods, dynamic system behavior and heat pump design [15]. In calculation methods, fast and accurate

[2] After 2008
[3] TV, Computers, Lights and so on.

procedures with simplified performances are more interesting for the researchers, as many articles deal with simulation tools like TRNSYS, ESP-r [12], [31], [32]. For the analysis of the dynamic system, a more detailed approach is necessary, as changes of the physical system over time, such as weather changes or user behavior, influence the behavior of HPs. [15].

The focus of this research is on the dynamic behavior modeling of the HPs in the residential applications.

3.2. Heat Pump Modeling

HPs extract the low temperature heat from the ambient and convert heat it up to the higher desired temperature [15]. HPs provide an efficient alternative to fossil fuels or electric heaters. The electric heater converts all of the input electrical power to thermal energy [33]. The efficiency of the HPs is higher; it is described by the coefficient of performance (COP)[4]:

$$COP = \frac{Q_{thermal}}{P_{electrical}} \tag{18}$$

In equation (18), $Q_{thermal}$ shows an effective heat transfer of the condenser and $P_{electrical}$ represents the input electrical power of the compressor. From thermodynamic point of view, the HP gets its primary energy from the compressor, releases the absorbed heat to the condenser, and turns back to the evaporator after expansion through the valve. The most efficient HPs have the COP around 4-6 which means that the primary energy for heating is building significantly reduced compared to conventional methods [33].

The first studies on dynamic modeling of TCLs have been done in [34]. For this study, a mathematical modeling of the system is implemented neglecting the furniture and internal gains. This simple model has been used in further studies. In [35], a mathematical model for user behavior is introduced and mainly discusses the system in physical pattern. Here, the process states have some issues and a precise stochastic function is necessary for the modeling. An economic model predictive controller with perfect forecasting is presented based on thermodynamic equations of the HPs [26]. In this thesis, the states of an aggregated HP model are used to describe the dynamic behavior of a heating/cooling system. This model extracted [36], [37] describes the transition states with physical models of thermostatic loads. Further, we develop a simple model for the building to show the consumer behavior and the corresponding changes in the output power of HPs. The thermal model shown in Figure 11 represents the configuration of the loads and thermal sources in a typical house.

[4] COP of Resistance Electrical Heater is 1, whereas in our case model COP is assumed 3.

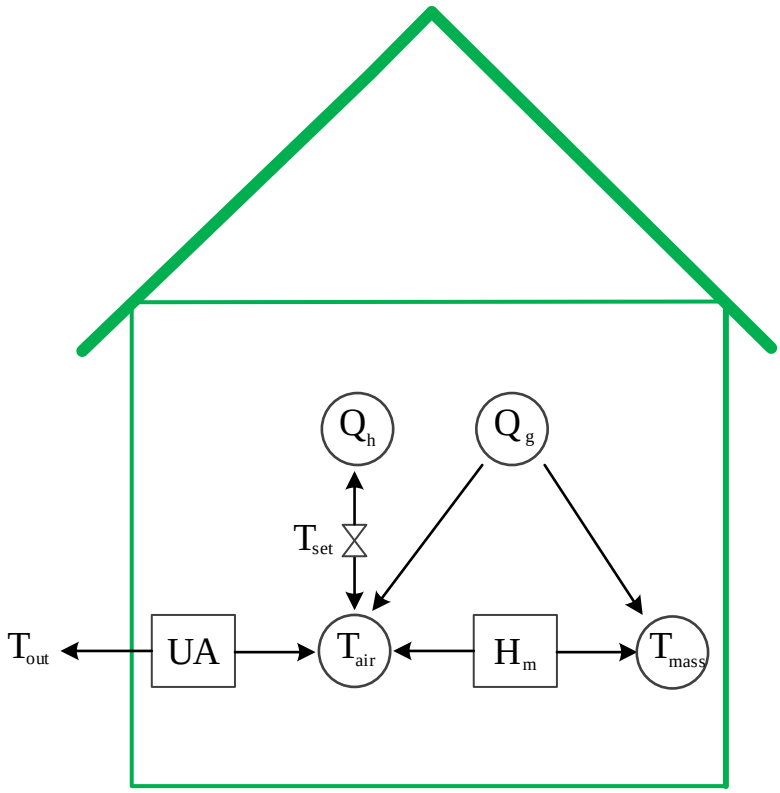

Figure 11: Thermal model of home heating/cooling system

In this model, H_m is the thermal coupling between the air and the mass inside the buildings, assumed to be perfect coupling, so it is negligible for the model simplifications. The principle relations in the model in equations (19) and (20) shown:

$$r_{off} = \frac{UA(T_{out} - T_{set}) + Q_g}{C_a + C_m} \tag{19}$$

$$r_{on} = r_{off} + \frac{Q_h}{C_a + C_m} \tag{20}$$

Here, r_{off} and r_{on} describe the rates of heating/cooling and air temperatures in $°C/h$. The given thermostat dead band is needed for adequate control. UA[5] represents the conductance of the building and Q_g is thermal gain through the solar and internal loads. C_a and C_m are thermal mass of the air and building materials furnishings, respectively.

[5] Overall Heat Transfer Coefficient

$$\varphi = \frac{r_{off}}{r_{off} + r_{on}} \tag{21}$$

In order to get more feasible parameters [37], the duty cycle (21) is presented. The time-independent coefficient on population diversity helps to solve the state space equations of the device. Without the loss of generality, it can be assumed:

$$r_{off} + r_{on} = 1 \tag{22}$$

According to this physical model, a state space model representing of the state transitions is extracted. The states are defined for heating/cooling device as ON/OFF modes. Next, each state is divided in two parts, Satisfied and Unsatisfied condition. The device can be in any of these four states. As shown in Figure 12, the Satisfied/Unsatisfied conditions are defined according to the application type (heating/cooling) [36]. For example, the objective of a cooling device is to keep the temperature below a certain set point. Thus, a temperature below the set point temperature means the device is in satisfied condition, while a temperature above the set point is stated as unsatisfied condition. In the contrary case, in heating mode, the satisfied condition is fulfilled if the temperature is above the set point and the unsatisfied condition refers to a temperature below the set point. The quotations are summarized in Figure 12 and the focus of this thesis is only in the heating mode:

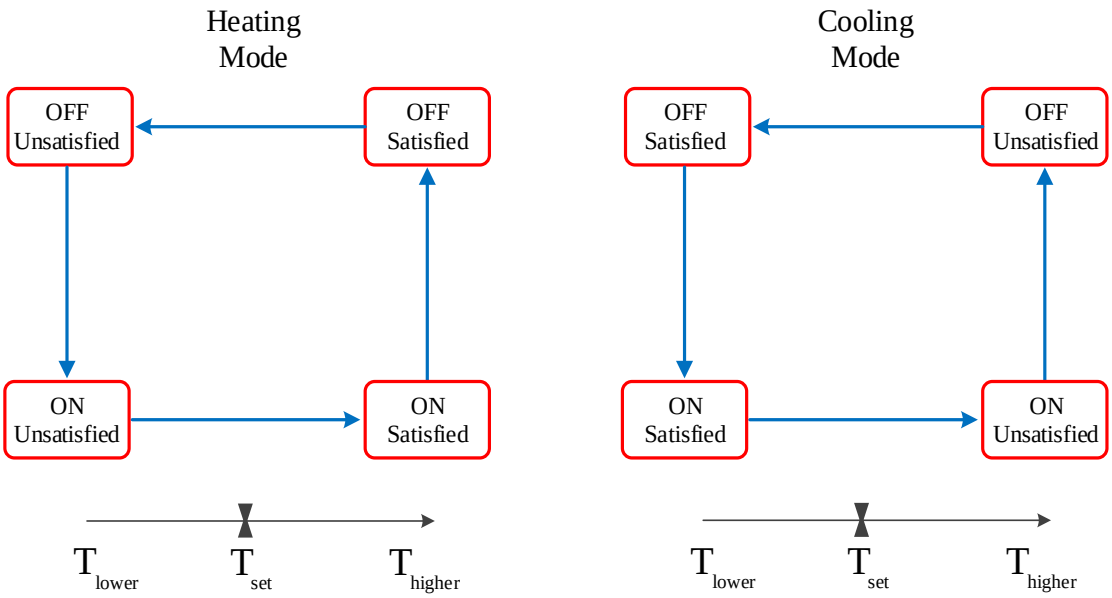

Figure 12: Schematics of state transitions in heating/cooling modes

In heating mode, the transitions between the OFF and ON modes are described below:

$$\dot{N}_{off}^{UN} = -\varphi \dot{N}_{off}^{UN} + \varphi \dot{N}_{off}^{S} \tag{23}$$

$$\dot{N}_{off}^{S} = -\varphi \dot{N}_{off}^{S} + (1-\varphi)\dot{N}_{on}^{S} \tag{24}$$

$$\dot{N}_{on}^{US} = \varphi \dot{N}_{off}^{US} - (1-\varphi)\dot{N}_{on}^{US} \tag{25}$$

$$\dot{N}_{on}^{S} = (1-\varphi)\dot{N}_{on}^{US} - (1-\varphi)\dot{N}_{on}^{S} \tag{26}$$

By applying the state space representation and deriving matrix A from (23) to (26), the state transitions without DR are shown in (27) and (28):

$$\dot{x}(t) = Ax(t) \tag{27}$$

$$x(t) = \begin{bmatrix} N_{off}^{UN} \\ N_{off}^{S} \\ N_{on}^{US} \\ N_{on}^{S} \end{bmatrix}; A = \begin{bmatrix} -\varphi & \varphi & 0 & 0 \\ 0 & -\varphi & 0 & 1-\varphi \\ \varphi & 0 & \varphi-1 & 0 \\ 0 & 0 & 1-\varphi & \varphi-1 \end{bmatrix} \tag{28}$$

So far, the physical parameters for modeling the HP components are applied. At this level, to make the system more precise, the effects of demand behavior and stalling phenomena are added as shown in Figure 13. As soon as the HP is switched on, the hot water in the tank is replaced by cold water from the bottom of the tank. The fraction of ON devices which shows the power demands is represented by η. On the other hand, the tank has different layers of hot and cold water. Depending on the relative rates of heat that comes in or goes out, the temperature levels in the tank goes up or down. This fact is called stalling phenomena and represented by ρ [37].

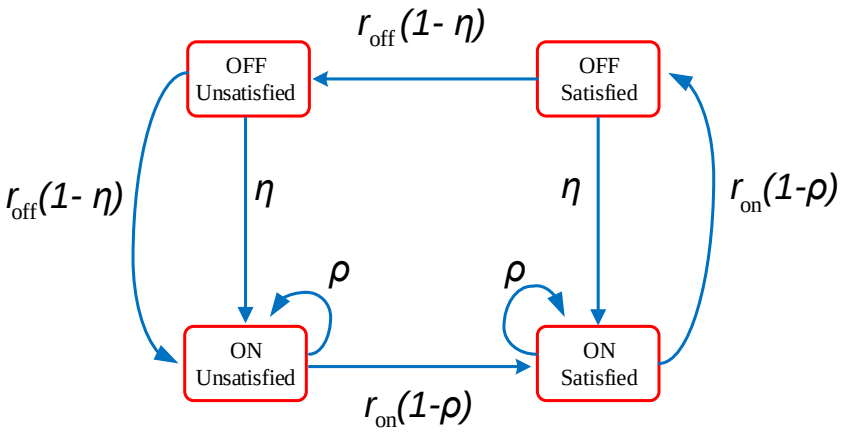

Figure 13: State transition diagrams for heating model

By manipulating the above relation and applying the mentioned effects based on [36], [37] the following state space equations are obtained (29):

$$x(t)=\begin{bmatrix} N_{off}^{UN} \\ N_{off}^{S} \\ N_{on}^{US} \\ N_{on}^{S} \end{bmatrix}; A=\begin{bmatrix} -\varphi(1-\eta)-\eta & \varphi(1-\eta) & 0 & 0 \\ 0 & -\varphi(1-\eta)-\eta & 0 & (1-\varphi)(1-\rho) \\ \varphi(1-\eta)+\eta & 0 & (1-\varphi)(1-\rho) & 0 \\ 0 & \eta & (1-\varphi)(1-\rho) & -(1-\varphi)(1-\rho) \end{bmatrix} \tag{29}$$

The advantage of this method is the simple description of DR programs like Direct Control Load (DLC) [37]. The state transitions show the probability density of the HPs in OFF/ON modes based on the duty cycles and end-user behaviors.

Different scenarios of the dynamic behavior of HPs without DR can be found in Appendix C. In the chapter 3, the proposing the controlled approach in existence of DR will be presented.

3.3. Dynamic Behavior of the HP

The duty cycle of the building is described by the thermal equations in section 3.2. The duty cycle is used to create the propagate matrix for the dynamic state transitions. The dynamic model of HP is useful for the development and simulation of agent-based control approaches. This section is dedicated to the control of the end-users' dynamic behavior in over-riding. Figure 14 shows the physical system, the state space model and the control.

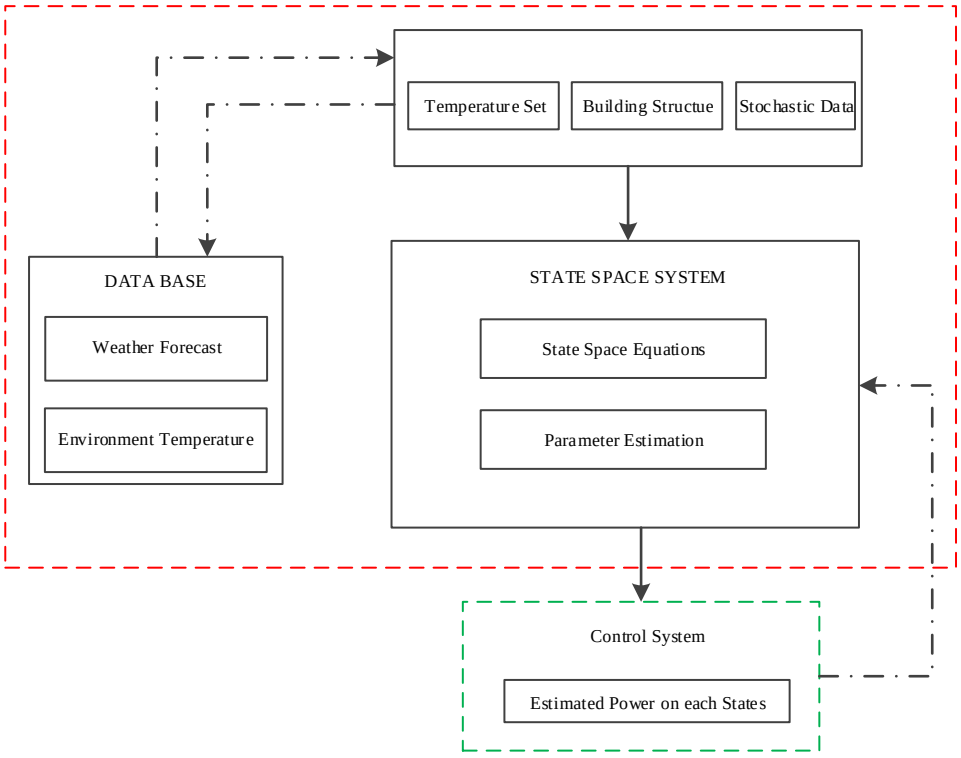

Figure 14: HP state space modeling and controlling

To include user behavior in the model, utility curtailments, and over-riding signals are represented as below:

$$B_1 = \begin{bmatrix} 0 \\ 0 \\ -\gamma \\ -\gamma \end{bmatrix}; B_2 = \begin{bmatrix} -\tau \\ 0 \\ 0 \\ 0 \end{bmatrix} \tag{30}$$

In general, the user behavior is unpredictable. Due to the general end-user tendency for decreasing the demands, matrix B_2 represents the utility curtailments. Matrix B_1 is introduced as an expression of over-riding behavior. The design parameters for the propagate and control matrix, which is abstracted from [36] can be found in Table 1:

Parameter	ρ	α	τ	γ
Value	10%	10%	10%	50%

Table 1: Design parameters for the dynamic behavior and controlling model in HPs

Assuming the typical values in European building system [38] the physical parameters for definition of the HP are presented in Table 2:

Parameters	**Values**	**Units**
Temperature	50	^{o}C
Thermal Capacitance (Air)	1.1	kJ/kg.K
Thermal Capacitance (Building)	1.2	kJ/kg.K
Thermal Heat Gain	1.3	kJ/kg.K
Thermal Heat Gain by Devices	4	kJ/kg.K
Overall Heat Transfer Coefficient	1.2	kJ/kg.K

Table 2: Building physical characteristics

As mentioned before, duty cycle depends on physical parameters like set temperature, HPs output power and control methods. The duty cycle range is limited from 40% to 80%. We studied the model in two different cases:

1. Dynamic behavior of the system without DR
2. Dynamic behavior of the system with DR

For the first study, the dynamic behavior of the system without DR, two scenarios are implemented with:

1. Constant duty cycle
2. Variable duty cycle

In the constant duty cycle scenario, the simulations are accomplished with different initial states. The results show that independently from the initial states, the state transitions converge to the same natural equilibrium states, which occurs when the state transitions in ON and OFF modes are invariant. The simulations of the dynamic state are available in Appendix C.

In the variable duty cycle scenario, the model simulated for varieties of duty cycles (40%, 50%, 60%, and 70%) with constant initial states. The simulations of the dynamic states are available in Appendix C.

In the second case, the dynamic behavior of the system with DR is considered. The simulations show that matrix B_2 becomes instable and goes to infinite with any input step signal. Although all of the system poles[6] are negative, one of the poles is very close to zero, which leads to conditional system stability.

$$M = [B \quad AB \quad AB^2 \quad AB^3] \tag{31}$$

In equation (31), M represents the controllability matrix. The controllability matrix has full rank, which means the system is potentially controllable. Applying the method proposed in [36] and the Ackermann method, the system was stabilized. The user behavior, modeled as over-ride input signal, is viewed as unknown control input, which tracks the dynamic behavior responses of the plant. The close-loop feedback in the system helps the controller for converging state transitions to the natural equilibrium states.

By using the Ackermann method with the coefficients in (32), the system is controllable by the control signals (5%, 10%, 15%, and 20%). According to the control signals, system responses are evaluated for duty cycle of 40% under different levels of utility over-ride (5%, 10%, 15%, and 20%).

$$P = [-1.95 \quad -1.95 \quad -0.1 \quad -1.55] \tag{32}$$

[6] Eigen Values

The steady-state results are introduced in Table 3 and Table 4.

Single Impulse	5%	10%	15%	20%
OFF-Unsatisfied	+1%	+2%	+2%	+4%
OFF-Satisfied	+2%	+4%	+5%	+4%
ON-Unsatisfied	-2%	-2%	-3%	-3%
ON-Satisfied	-1%	-4%	-4%	-5%

Table 3: State transitions from the natural equilibrium for $\varphi = 40\%$ with DR

In this part, for the development of the aggregated control model for the HPs, we consider the large population of TCLs shown in Table 4.

Single Impulse	5%	10%	15%	20%
OFF	+3%	+6%	+7%	+8%
ON	-3%	-6%	-7%	-8%

Table 4: ON/OFF transitions from the natural equilibrium for $\varphi = 40\%$ with DR

4. Micro Combined Heat and Power

4.1. Introduction

Combined Heat and Power is a technology for cogeneration of useful heat and power simultaneously by industrial process or small power plants. Small power generation that has received increasing attention as a viable alternative production in distribution systems is called Micro Combined Heat and Power (CHP) Cost saving, emission reduction, smooth operation, control possibility are the primary benefits of the CHP [17], [39]. However, the most important advantage of the CHP compared to conventional power plants is the potential of high efficiency due to low losses of Exergy[7] destruction.

This technology is used in a low voltage level for self-consumption. Furthermore, the excess electrical power can be fed into the grid and dispatched to the neighborhoods. Besides, the heat generated by CHP is used for self-consumption of the building like DHW and Space Heating [40].

The most common technologies for CHP in world markets are SM, FC, GT, ICE, ORC (Organic Rankine Cycle), Reciprocating Engines and Steam Cells [41] as a prime mover. For the technologies of reciprocating Engines, SM, ICE, and GT technologies, natural gas containing 85% methane is used as a fuel.

In FC technologies, usually the natural gas is mixed with WGS (Water Gas Shifting) reactions to produce pure hydrogen as a fuel of the FC. High temperature SOFC and low temperature PEMFC are the most typical FC technologies used in urban areas.

The principle of CHP to generate heat and power simultaneously is useful in residential buildings, as the generated electrical energy can be used directly to supply the electrical devices.

[7] Maximum useful work possible during a process that brings the system into equilibrium with a heat reservoir

The produced heat can be used for space heating or stored for domestic hot water applications. There are different types of configuration for heating demand in residential applications.

There are different CHP configurations with and without storage for residential applications. In northern countries of Europe for DHW applications the numbers of the CHP, which are equipped with storage tank are rising because of its ease of use. The schematic in Figure 15 shows the configuration of CHP which are equipped with tank storage for DWH supplies and space heating. In this work, we assumed this schematic for CHP operation.

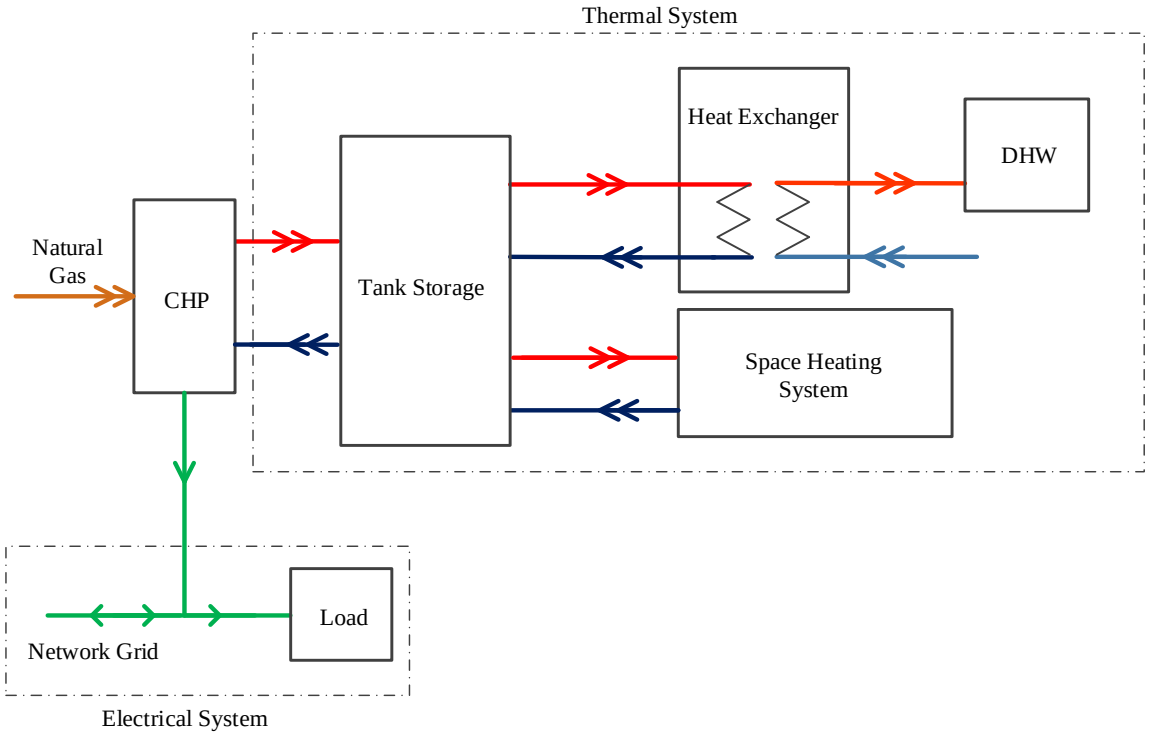

Figure 15: CHP configuration equipped with domestic hot water and space heating

4.1.1. Minimum Duration of Operation

In this section, the technical constraints of electrical and thermal energy generations for the model are explained. The CHP system usually consists of two main components: prime mover and auxiliary heater.

The prime mover converts the energy through combustion or chemical reactions to thermal and electrical energy. SM, FC, and ICE are the most common prime mover technologies. The research focuses on SM and FC technologies; ICE is ignored because of its high NOx emission.

Although SM are on the border of the demonstration phase and market phase, they are expected to be strong represented on the market in the future, due to the high flexibility, high heat to power ratio, low emissions, low maintenance and low noise level[8] [41].

Operational FC systems have demonstrated superior performance to combustion-based generation technologies. Owing to their lower emissions and higher performance and considering the recent tendency to micro-scale power generation systems, the viability of utilization of FC based cogeneration plants has been extensively studied in the recent years. As mentioned before, PEMFC and SOFC are the most common technologies for using in prime mover of the CHP. On the other hand, low temperature PEMFC (80°C) which requires the pure hydrogen as fuel and high temperature SOFC (800°C) needs internal reforming. These characteristics create some implementation challenges of the FC technologies in residential usage. For these reasons, the application of the technology for residential application is still in R&D phase[9] [42].

CHPs are not designed for starting-up or shutting down continually. SMs have quick start-up and short cool-down periods and the CHP systems are limited by the minimum duration of operation [43]. It means the CHP unit is locked to avoid frequent switching. The minimum duration of operation of 30 minutes for SM technology and 45 minutes for FC technology are reported [42], [44].

[8] Solo, WhisperTech are the famous companies for CHP production in SM technology
[9] Ceres Power company is famous company for CHP production in FC technology

Figure 16 shows the minimum duration of operation for SM and FC technologies. Zero start-up in this figure shows the time of switching and necessarily starts at zero hour.

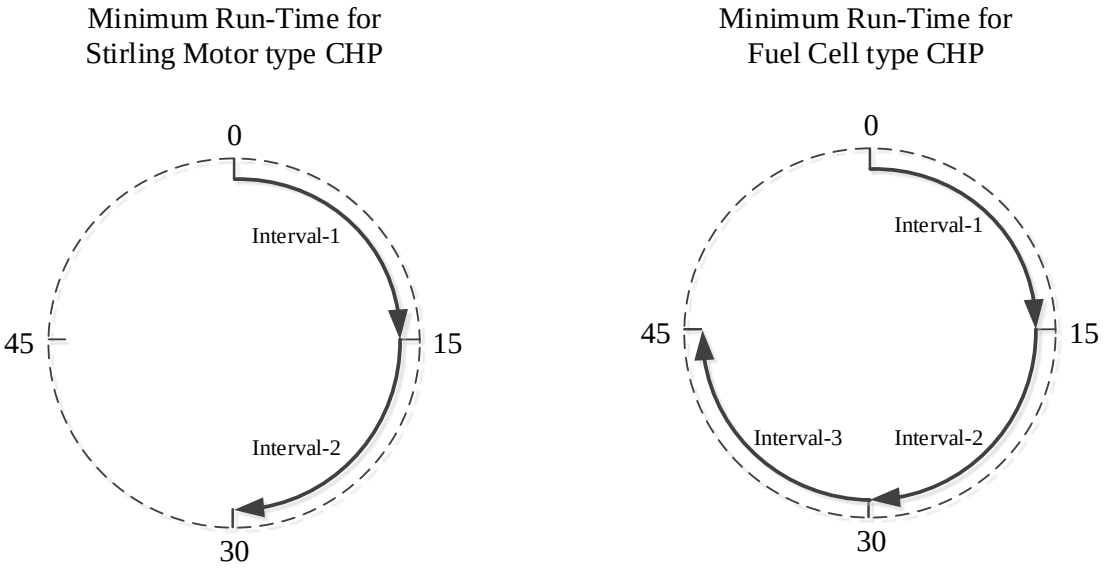

Figure 16: Minimum duration of operation for SM and FC technologies of CHP

4.1.2. Thermal Generation and Storage

As described before, CHP systems in residential applications are usually equipped with a thermal storage tank used to store hot water for the building. The tank storage has four temperature layers, shown in Figure 17. The top and third layers belong to the prime mover working and store the hot water in the specific temperature range. When the prime mover starts its operation, the CHP control tries to keep the energy generation in the range between 88°C to 55°C.

The second and fourth layers belong to auxiliary heater. The auxiliary is switched as soon as the temperature of top layer drops below 60°C and the prime mover operation is restricted. The auxiliary heater is switched on again if the temperature drops below 50°C.

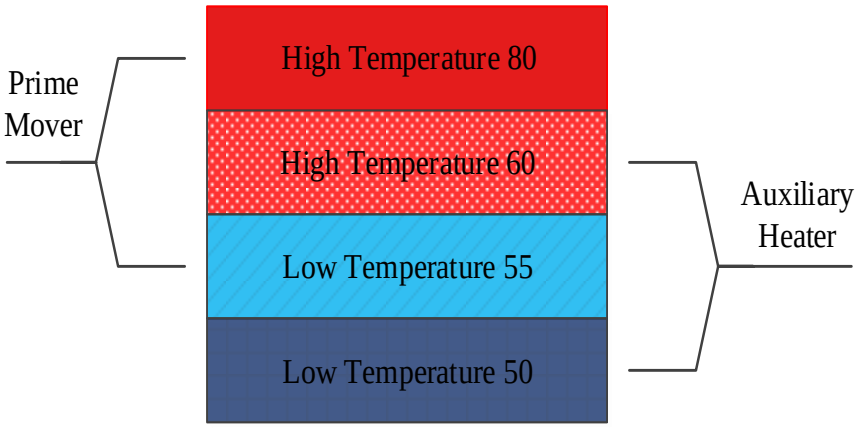

Figure 17: Tank storage temperature levels

On the other hand, the energy retailer sells the electricity to the household and buys the exported electrical energy from the household. The electrical energy balance for CHP system is followed by (33):

$$e_{production} + e_{in} = e_d + e_{out} \tag{33}$$

where $e_{production}$ represents produced electrical energy by the CHP and e_d is the electrical demand. In this equation, e_{out} is exported excess of generated energy, e_{in} is the imported

energy from the grid. The complete primary energy of the CHP can be converted to heat and electricity form by the following equation:

$$k = \frac{\eta_{thermal}}{\eta_e} = 4 \tag{34}$$

In equation (34), $\eta_{thermal}$ and η_e represent the thermal and electrical efficiency of the CHP conversion. This means, during CHP operation, 80%[10] of the primary energy is converted to heat and 20% to electrical energy. With SOFC technology, the coefficient is 3, 60%[11] of primary energy is converted to heat and 40% to electricity. In this thesis, the CHP losses are neglected. The enthalpy changes account for thermal transferring is followed by (35):

$$h = mC\Delta T \tag{35}$$

In equation (35), m is a mass flow rate of water that circulates throughout the system, for this model it is assumed to be 200 kg. Typically, mass flow rates for residential applications are in the range between 100kg and 100 kg [44]. C is the specific heat of the water, it is assumed to be 4.18 $kJ/kg.°C$. The temperature difference is calculated for each layer with respect to the reference temperature 25°C. On behalf of the complement of equation (35), higher and lower amount of the CHP's energy calculated through (36) and (37). Equations (36)-(38) show the limitations for the prime mover of the CHP. The control system always tries to keep prime mover generation in this range based on equation (38)

$$h_{low,CHP} = mC(T_{low,CHP} - T_{ref}) \tag{36}$$

$$h_{high,CHP} = mC(T_{high,CHP} - T_{ref}) \tag{37}$$

$$h_{low,CHP} \le h_{prime\_mover} \le h_{high,CHP} \tag{38}$$

Equation (39) shows that the operation of the auxiliary heater is limited between the maximum and minimum temperature range. The temperature range of the auxiliary heater was introduced in Figure 17.

[10] Typical thermal efficiency in SM is 80-90%
[11] Typical thermal efficiency in FC is 60-70%

$$h_{aux,\min} \leq h_{aux} \leq h_{aux,\max} \tag{39}$$

The local control system according to the minimum duration of operation constraints (introduced in section 4.1.1) and the enthalpy changes constraints, calculates the flexibility of the CHP operation. The aim of the CHP control is to keep the device operating as long as possible. The control switches off immediately if the temperature rises above the higher temperature limit of the storage. Otherwise, if the water is heated above the high-temperature limit, it converts to steam. Analogically, if the temperature drops below the range below the lower limit, the auxiliary heater is switched on.

To summarize, the CHP operates in specific operation limits according to the higher and lower temperature limits of the tank storage as Figure 18. Within this operation limits, CHPs are not allowed operating at any arbitrary node and it depends on the conditions of operation line. The initial point of the operating line denotes by the requested electrical energy on x-axis and the current temperature of the storage on y-axis. The requested electrical energy can be assigned by the operator (Aggregator Agent or Household), which is always restricted between zero and the maximum nominal electrical power of the CHP. The slope of the line is always constant and depends on heat to power ratio in equation (34).

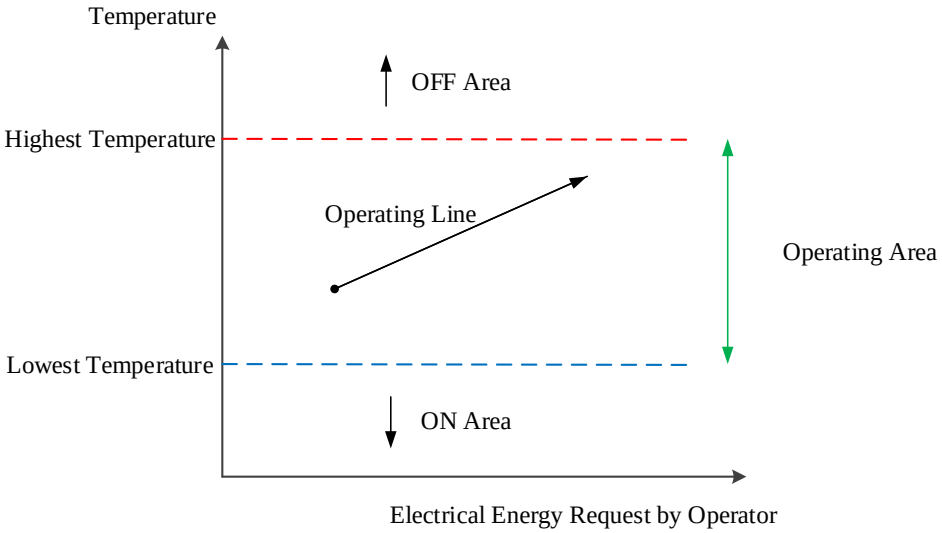

Figure 18: CHP operation area

In other words, the flexibility of the CHP operation in distribution system depends on the volume of the storage tank and thermal demand of the building. If the thermal demand or volume of the tank storage increases, the CHP can generate more electrical power. The single-

CHP algorithm that tracks the availability of the CHP operation to the grid is shown in Figure 19. CHP is triggered based on minimum duration of operation and assigned electrical and thermal demand. The first goal step of the control system is to match the electrical demand with the electricity generation of the CHP. The control system checks the technical constraints for the CHP availability. After running the algorithm, the thermal storage capacity (State of Charge) updated to the new temperature point. In addition, the local controller sends the amount of exported electrical power to the network grid.

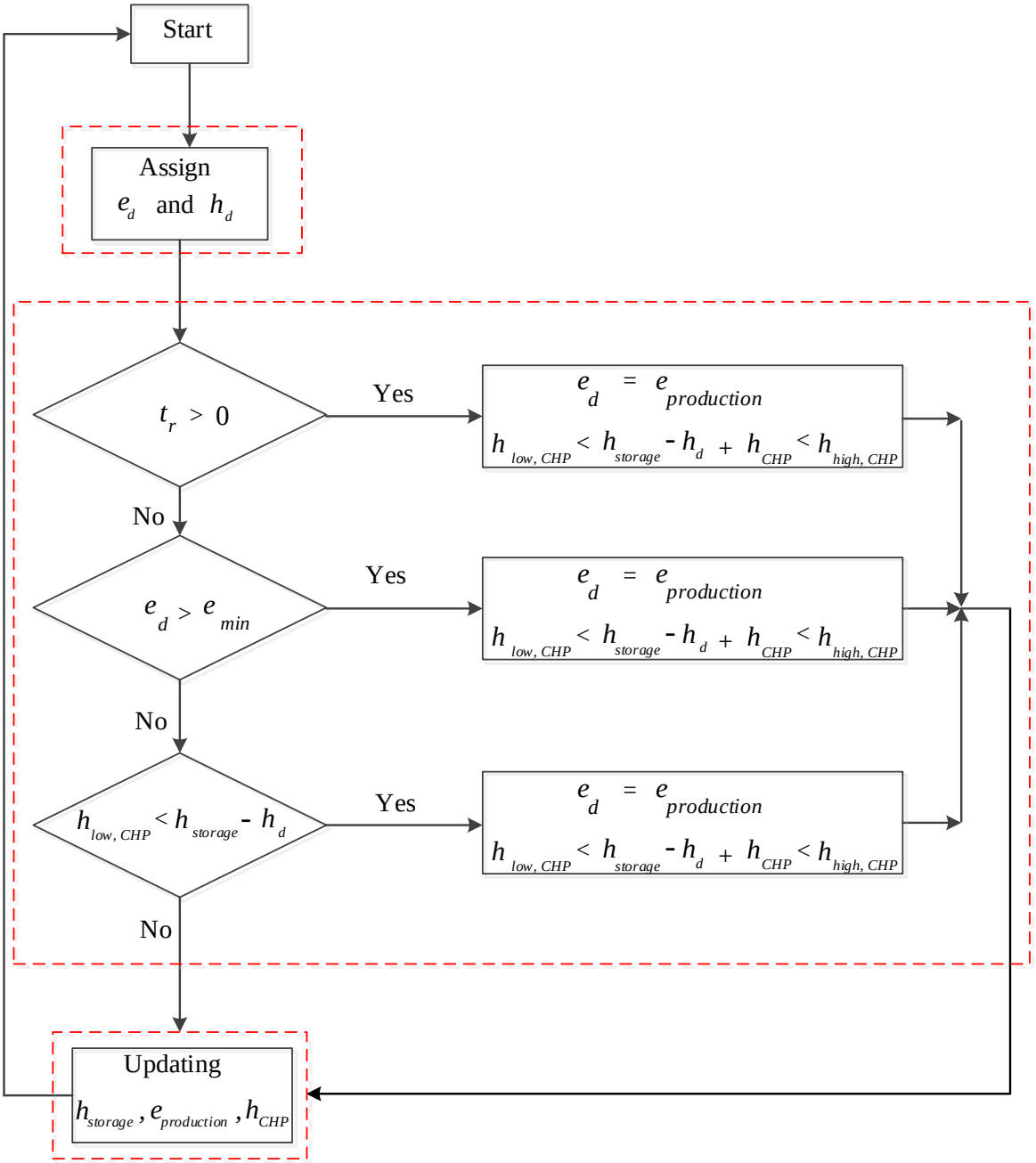

Figure 19: Algorithm for controlling electrical generation in single CHP operation

When the possibility for extra generation is confirmed by the households (or a third party), the network operator's task is to determine how the CHPs should dispatch the generation in the grid. In the presence of only one CHP, the grid operator does not have multiple solutions for dispatching the generations among the loads. However, as the number of CHP in distribution level increases, the role of the grid operator is highlighted. Based on different control methods, the grid operator can choose the optimum solution(s) for the dispatch of CHP's generation. The interaction of the algorithm with physical system based on DR actions is shown in Figure 20.

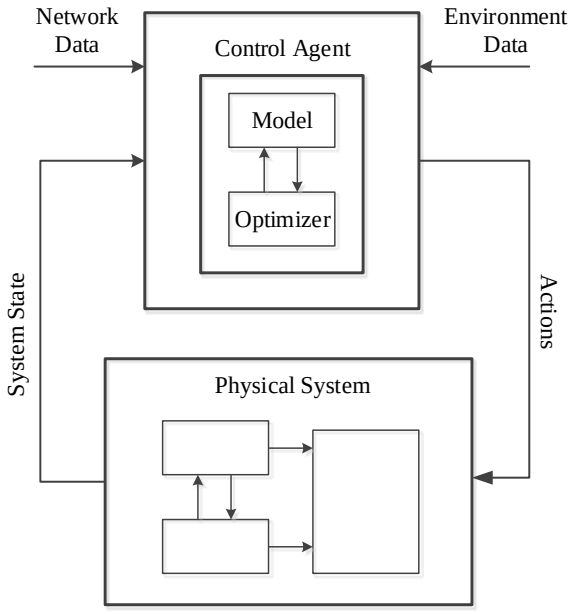

Figure 20: Controlling approach for the CHP

5. Agent-Based Control

5.1. Introduction

The transition of conventional power system into the flexible smart grids requires impressive control system. The need for autonomous control approach for complex power systems is increasing. Autonomous approach returns to the technique, which does not require human supervision or monitoring [45]. The control system should satisfy the flexibility, re-usability, robustness, and scalability as long as considering of technical constraints like time delay, global consistency, and uncertainty inference [46]. The most common methods for controlling the complex power system are categorized as below:

1. Centralized

2. Distributed

The centralized control is characterized by dominant part acts as a master, while the other parts act as servants. The master processes the information and sends signals to the slaves. Figure 21 shows the centralized control structure of single-agent that coordinates all the other participants. In centralized approach, there is only one core for decision making to achieve the global optimization point; however, in practice due to the existence of traffic data, delays, high computation power of the core entity, it has low efficiency. Besides, if the master is damaged the whole system will be out of control [47].

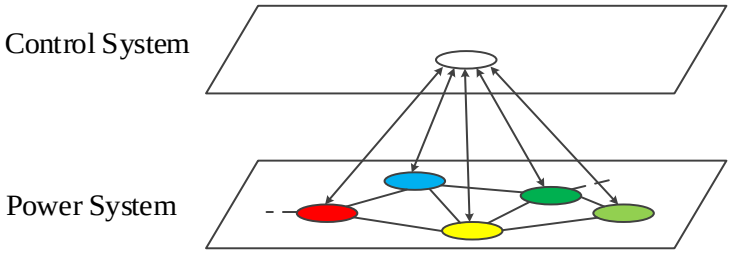

Figure 21: Centralized control structure

Distributed control approach is classified in two groups:

1. Conventional Distributed (CA/NA)

2. Modern Distributed (Agent-Base)

The conventional distributed process, which is also called completely Accurate/ Nearly Autonomous (CA/NA), has local database. This approach contains appropriate capability to solve the overall problem without any assistance of the other nodes. This control method is viewed as extended centralized control with distributed computations due to high cost for communications and implementations and difficulties to guarantee the local database consistency [48]. In this thesis, the focus is only on the modern distributed approach, which is also called agent-based control.

An agent-base control is an effective mechanism for autonomous controlling of the complex distribution system. Control agents employ cyclic process to accomplish the desirable tasks. Estimation, planning, and execution are the main three steps in the control cycle. Estimation uses the limited observation to compute the states. Planning gets the dynamic states from the estimation and by involving the constraints, produces an action plan for execution [49].

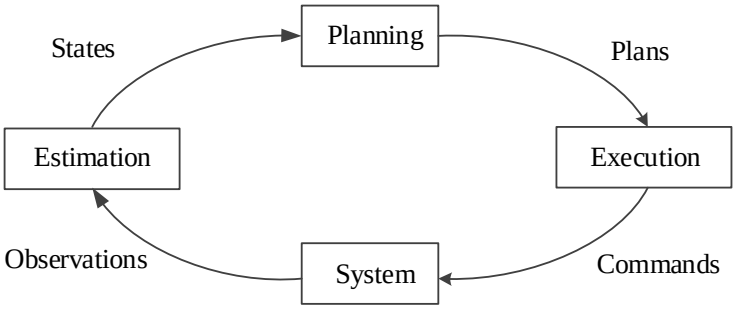

Figure 22: Cyclic process of control agent

In agent-based system, the agents usually collect the information from the surrounding by the local sensors. The input information is the raw data, which the agent should process. After organization, the data is analyzed for a decision in order to satisfy the global objectives of the system. Finally, the processed data should be transmitted to the local actuators as a new command [46].

5.2. Multi-Agent System

A large power system is decomposed to numerous agents, while agents that collaborate and communicate with each other are relatively independent. This technique that several agents cooperate to form a society is called Multi-Agent System (MAS) [47]. Easier implementation, increased robustness to uncertainties, enhanced adaptability compared to standardized design problems, are the most advantages in MAS approach.

Compared to the operation of centralized systems, MAS provides more feasible solutions and not necessarily the optical solution [48]. The development of a generalized framework for the testing of control system design is one of the most important challenges in MAS. As shown in Figure 23, each local MAS cooperates each other to operate in the whole system as an entity.

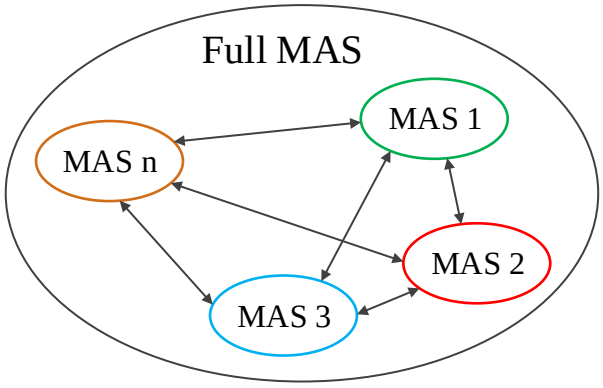

Figure 23: Organization of the full MAS system

MAS usually is divided to two typical architectures:

1. Distributed

2. Decentralized.

In distributed architectures, the agents receive the information, analyze, and take decisions independently. The agents also have the authority to communicate with agents at the same level to achieve own or team-oriented goals. Figure 24 shows the simple schematic of distributed control structure, in which the agents cooperate to achieve the common goals.

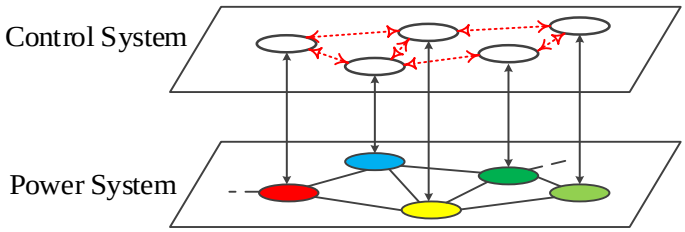

Figure 24: Agent-base control with distributed structure

On the other hand, in decentralized approach the agents do not have data exchanging with same level agents. They control their own group according to their defined strategies. The results of the coordination and decision making is submitted to aggregate agent in upper layer [49]. Figure 25 depicts the general configuration of decentralized system that agents do not have direct communication together.

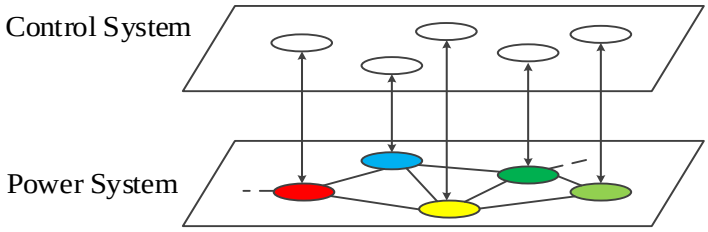

Figure 25: Agent-base control with decentralized structure

There are many types of architecture of agent-based control of different applications. Broadly speaking, the most important MAS architectures are:

1. Flat
2. Module
3. Hierarchical

A flat organization of MAS implies that each agent can directly contact any of the other agents. The agents stand in parallel and operate independently. Also, no control of one agent by another agent is allowed which creates dynamic adjustments of MAS organization to change the tasks

and environment [50]. This architecture satisfies the communication, reliability, and coordination of the control system.

Figure 26: Flat architecture

Module architecture divides the whole system in several modules. Each module can communicate directly with other modules through the common interface. The autonomous decision and simpler communication design are the most important characteristics of module architecture [48]. This architecture increases efficiency of task execution and reduces communication overhead. Also, within each module high flexibility similar to flat organization flexibility is usually enabled [50]. High level of autonomy and reliability are the most characteristics of module architecture.

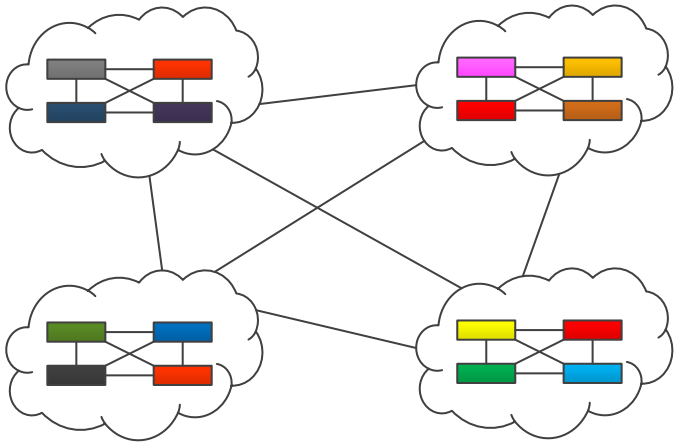

Figure 27: Module architecture

Hierarchical, is natural way for decomposing the system to the smaller groups. It provides efficient communication networks and decreases network complexity [49] and there is no need for a mechanism for agent location. Disadvantage of this configuration is that lower level depends on higher level and whenever the data are lost between the higher and lower levels,

lower level interacts with default values without inputs from higher level. Again, local optimization of the part of the network does not necessarily mean the overall system is operating on optimum way [18].

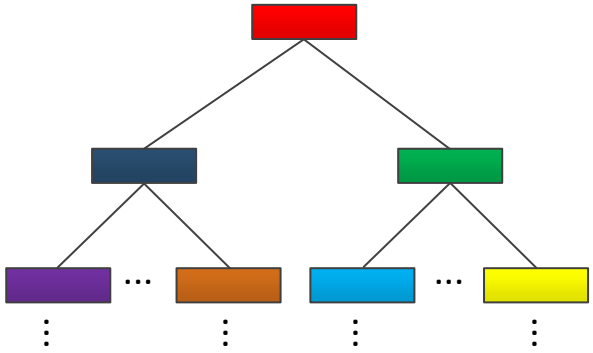

Figure 28: Hierarchical architecture

All these three architectures could be useful for decentralized approach and have their specific features. The features are summarized in Table 5:

Type	Flat Architecture	Hierarchicel Architecture	Module Architecture
Structure Complexity	Fair	Best	Good
Communication Complexity	Fair	Best	Fair
Coordination Complexity	Fair	Best	Good
Autonomy	Best	Fair	Very Good
Reliabelity	Good	Fair	Very Good
Adabtabelity	Fair	Best	Very Good

Table 5: Common MAS architecture features

5.3. Control Method

As a case study, the cooperative control method for the 19 residential settlements in distribution grid is considered. Thirteen of them are purely passive loads. Five of the houses are equipped with PVs, and two of them with CHPs. It is assumed the power flow also can be injected through the fully two transformers. Distribution losses of the lines and cables are neglected. As shown in Figure 29, the distribution system is divided into three subgroups, which are called clusters. Each agent controls the cluster independently and the agents cooperate as MAS. Each agent has access to current consumption power of the end-users and the current generation of DER of grid. The agents have already received the optimum consumption schedules of the households by Day Ahead Market (DAM). The agents are responsible for the Supply and Demand Matching (SDM) actions with optimally using the electricity production [51], [52].

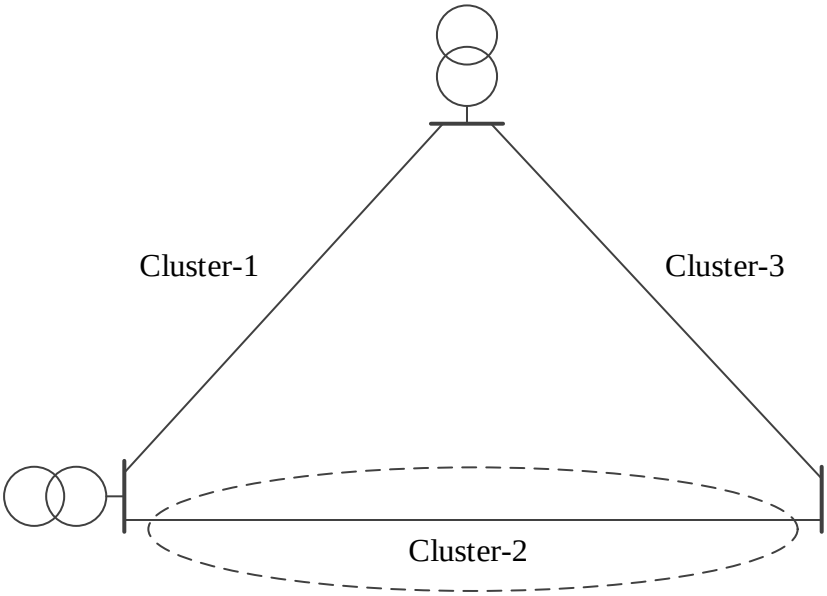

Figure 29: Case study of distribution system

Bidirectional power flow requires an effective mechanism to manage power flow in the distribution system due to RES contributions. In this thesis, NAN level the hierarchical architecture is used for the communication and control approach. The hierarchical architecture is selected due to its advantages in respect of structure, communication, and coordination;

however, its disadvantages are the reliability and autonomy. The clusters are allowed to inform each other regarding the excess or lack of energy. Figure 30 shows the different layers of hierarchical architecture.

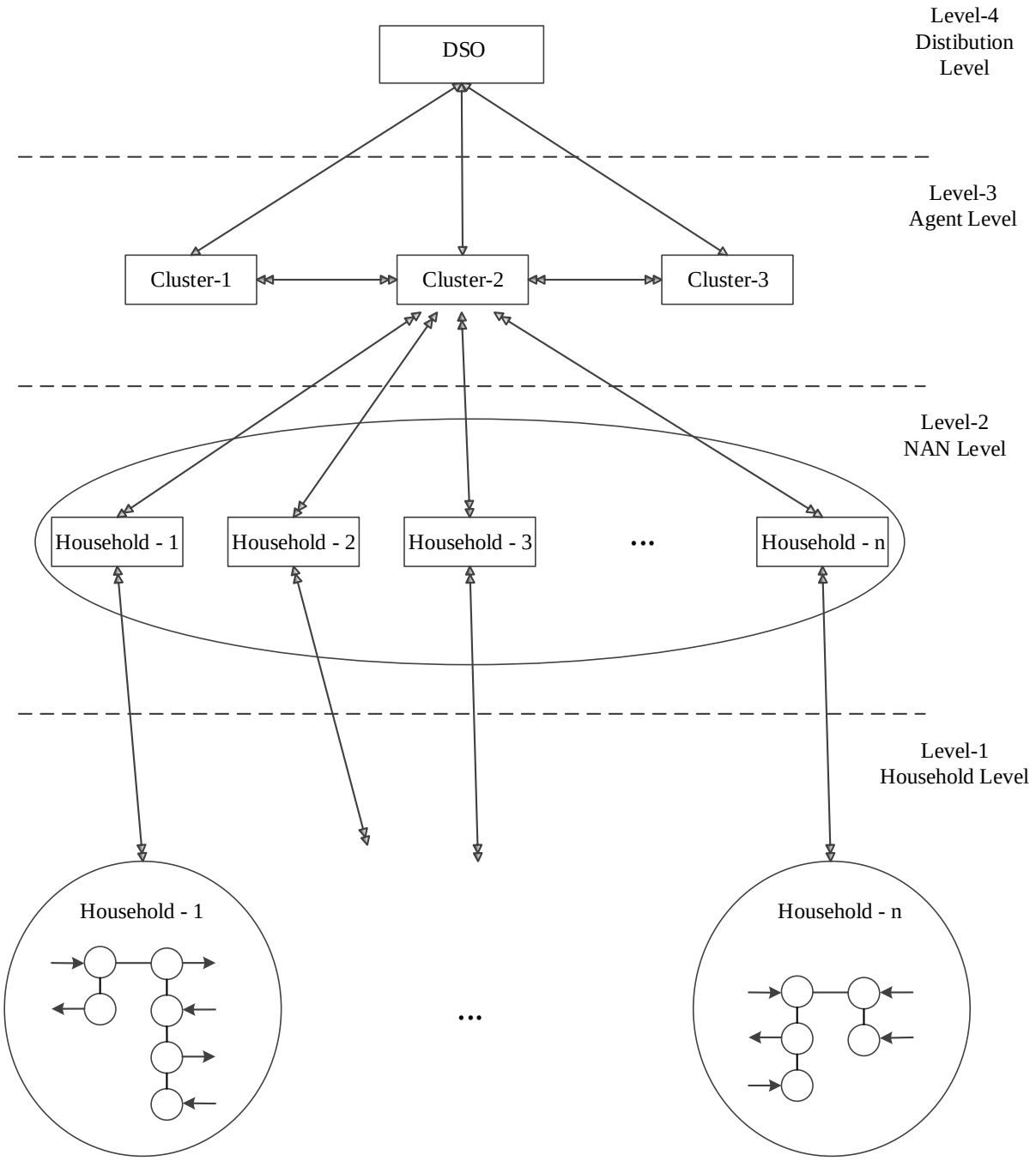

Figure 30: Infrastructures for autonomous distributed network

In the case study, the infrastructure of distribution system is organized as below:

1. Household
2. Neighborhood Area Network (NAN)
3. Cluster
4. Aggregated Agent

In household level, which is the lowest layer each household could be assumed as an independent agent for implementing its own strategies. Different controlling methodologies for Home Energy Management (HEM) are under developments. These approaches usually are applied the economical and marketing point of view for the controlling [53], [54]. In future, most houses will be equipped with energy boxes for the efficient management of home applications. The communication infrastructure for controlling the home applications is the fundamental requirement in this layer [55]. Figure 31 shows the typical HEM configuration. Here, we assume that each household transmits the optimum schedule for the cluster operator.

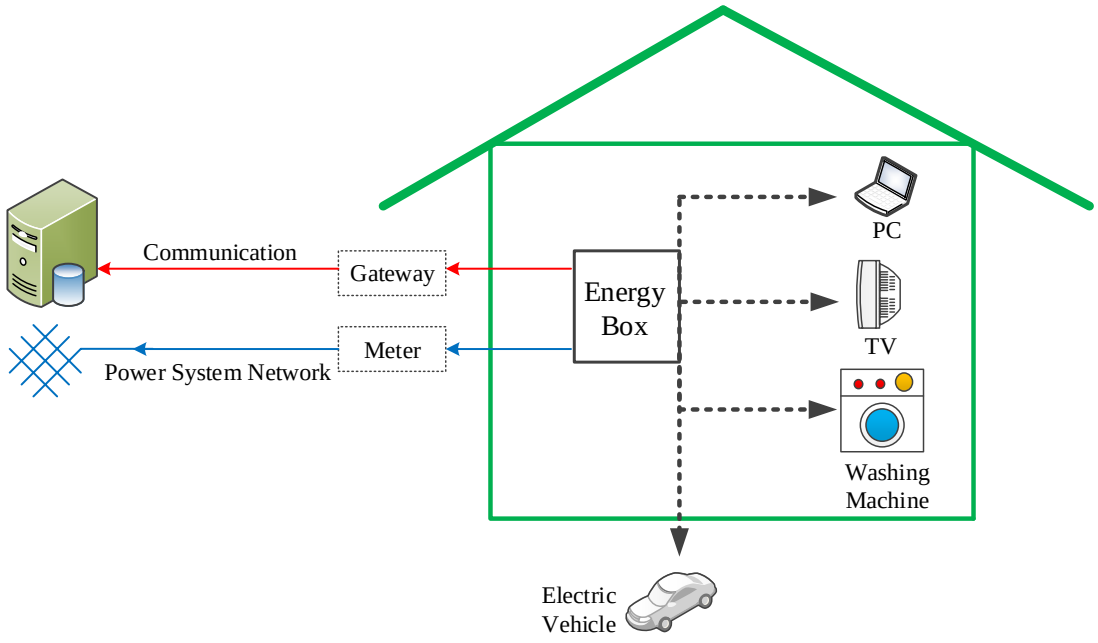

Figure 31: Schematic of HEM in future of the smart grid

In the second layer, passive household sends the current consumption to the corresponding cluster. The Active user transmits the current generation of the PV to the cluster. The cluster

tries to keep the aggregated schedule as close as possible to the DAM schedule. While the consumers devastates from the optimum schedule cluster operator applies the DIGOMIN[12] algorithm [56]. This algorithm, which is fully introduced in the next section searches for the optimal solution to compensate the deviations. The idea is to share the excess of generation inversely proportional to the deviated load's distance. The cluster operator has the authority to use the entire DER to compensate the deviations without any economy constraints.

In the cluster level, each agent cooperates in distributed pattern as shown in Figure 32. They can share the information regarding excess or lack of energy for further actions [48]. The results of their discussions are submitted to the aggregated agent. Finally, if the requirements are not fulfilled in the cluster level the aggregated agents apply the alternative solutions. The aggregator agents can sends a request to DSO or supply the rest of required energy through the other RES.

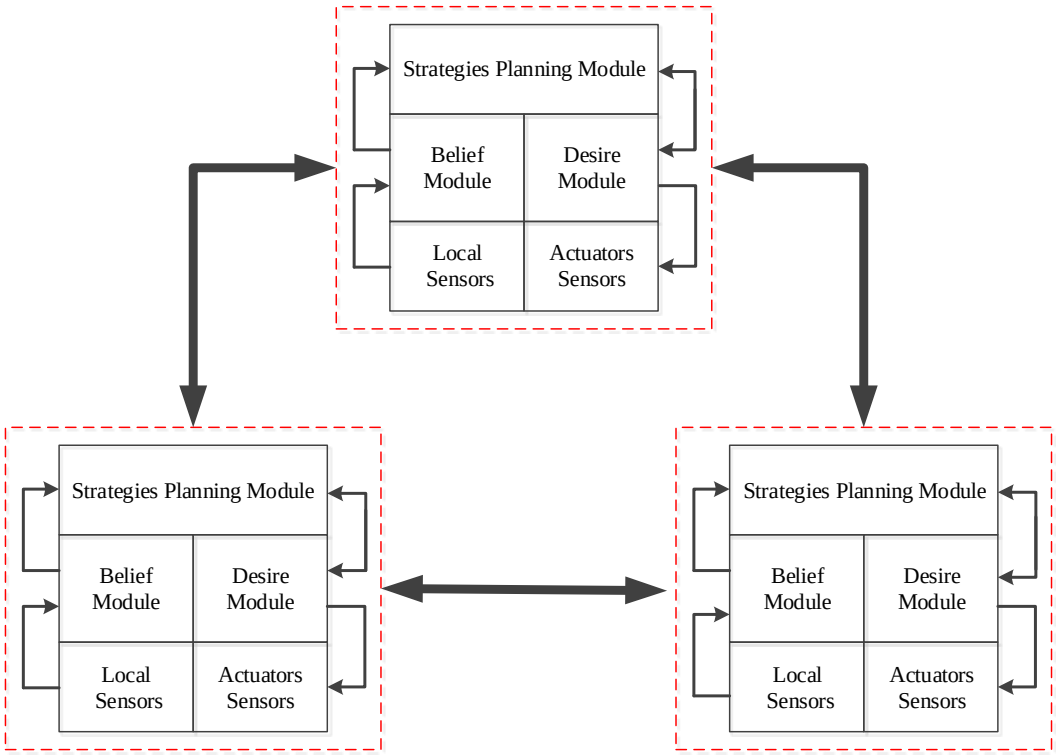

Figure 32: Distributed coordination of clusters for case study zone

[12] Dispatching the Generations Over the Deviations According to the Minimum Distance

5.4. Dispatching the Generations Over Deviations According to Minimum Distance

As mentioned before, each agent based on the own strategy tries to find the optimum solution(s) as soon as the deviations are detected. At medium voltage level, the centralized methods for generation dispatching are represented in [57], [58]. These centralized solutions are not applicable in distribution system level due to the high number of installed DGs. We are more interested to find alternative solutions to fulfill the technical constraints like voltage stabilization, hosting capacity, real-time controlling, and independency from network topology.

In this section, the cooperative control algorithm is presented. This algorithm shows how DERs dispatch the generation among the deviated households in an optimal way. For the distributed cooperative approach, every active node should supply the passive loads in inverse proportional relation to their distance. So in this thesis the contribution is called "Dispatching the Generations Over Deviations According to Minimum Distance"[13] [56]. The most important advantage of this approach is that only the distances between the nodes is required without any knowledge of the network topology [41], [45]. In other words, the algorithm is applicable for ring, radial, and network distribution patterns. In addition, this approach only needs the narrow bandwidth of the communication networks among the nodes.

$$S_m = P_m + jQ_m \tag{40}$$

$$S_n = P_n + jQ_n \tag{41}$$

Equation (40) shows the complex absorbed power by load that is indicated with m. Equation (41) shows the complex power, which is generated by RES. These sources are indexed with *n*.

Each household tries to follow the assigned schedule according to the DAM schedule. The deviations calculated according to (42):

$$\Delta\dot{S}_m^{\,0} = \dot{S}_m - \dot{S}_m^{\,0} = \Delta P_m + j\Delta Q_m \tag{42}$$

[13] In further sections we call this method DIGOMIN

In equation (42), $\dot{S}_m^0$ represents the absorbed complex power by the consumer according to the defined schedule. $\dot{S}_m$ shows the current consumption power of the consumer. Conversely, the deviated generation of RES is presented as below:

$$P_n^{residue} = P_n^{\max} - P_n \tag{43}$$

$$Q_n^{residue} = Q_n^{\max} - Q_n \tag{44}$$

Equations (43) and (44) show the excess generation or the flexibilities for producing more energy of DGs. The maximum delivered active and reactive powers of DERs are described by P_n^{max} and Q_n^{max}, respectively. Furthermore, $P_n^{residue}$ and $Q_n^{residue}$ are the deviations from the expected schedule.

$$P_m^n = \Delta P_m \frac{P_n^{res}}{d_m^n}\left(\sum_{n=1}^{N}\frac{P_n^{res}}{d_m^n}\right)^{-1}; Q_m^n = \Delta Q_m \frac{Q_n^{res}}{d_m^n}\left(\sum_{n=1}^{N}\frac{Q_n^{res}}{d_m^n}\right)^{-1} \tag{45}$$

In equation (45), P_m^n and Q_m^n are the contribution of an active and reactive node, respectively. In addition, this shows how the excess of generation is dispatched among the passive loads in an optimal way. Besides, d_m^n is the distance between the DG indicated by the index *n* and load deviations indexed with *m*. The similar quotations are suited for reactive power

5.5. Near-Neighborhood Compensation

So far, we modeled the grid components and represented the near-neighborhood method for optimal dispatching of the generation among the passive loads. The near-neighborhood approach is an efficient technique to increase the performance of the compensation procedure. Here, we introduce a scenario for applying DIGOMIN algorithm. A scenario for the load compensation is implemented in presence of PV, CHP, and HP as representatives of DER. The goal is to fully exploit the capability of DER for meeting the unexpected behaviors of the thermal and electrical load in the distribution system.

The priorities of scenario descriptions are followed as below:

1. Contribution of the PV generations
2. Contribution of CHP operation
3. Dynamic behavior of the HP by DR

First, the cluster agent compares the current PV generations with the assigned PV generation. The cluster operator compares between the aggregated schedules and current consumptions. Therefore, we will counter with four different cases as below:

States	Higher Consumption	Lower Consumption
Higher Generation	Check DIGOMIN algorithm	Positive Flag
Lower Generation	Negative Flag	Check DIGOMIN algorithm

Table 6: Load balancing states

If the aggregated current consumption is lower than the expected one and the aggregated current generations of PV is higher than the assigned schedule of DAM, the cluster has excess of generation. Figure 33 shows how the discovered deviations are compensated by PV.

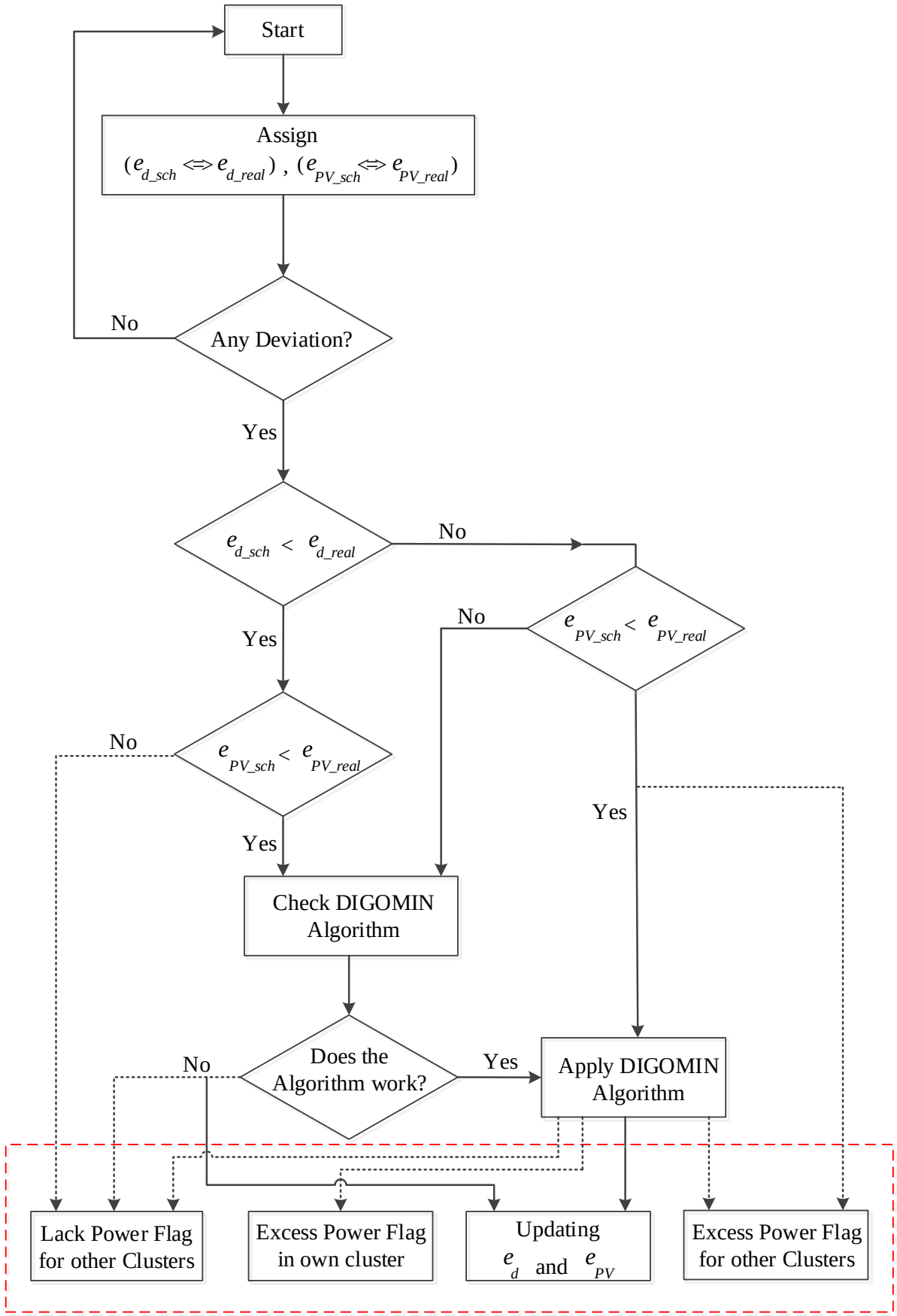

Figure 33: PV load balancing algorithm

The cluster is able to directly apply the DIGOMIN algorithm over the deviated loads and the rest of the energy could be dispatched for the next cluster. The current demand and generation values are updated.

If the aggregated consumption is higher than the expected values and the generation is lower than the forecasted, the cluster has lack of energy. At this point, the algorithm stops and the other clusters will be informed of the lack of energy; so, the DIGOMIN algorithm is not applicable. In the other two cases, the clusters check the availability for implementing the DIGOMIN algorithm.

In case the DIGOMIN algorithm can be applied, the current consumption power is updated. If the generation dispatch by the DIGOMIN algorithm is successful, the algorithm stops and the cluster transmits the updated values to the aggregator agent; otherwise, the second step of the algorithm starts. The cluster operator according to the availability of CHP operation tries to run the DIGOMIN algorithm. The CHP operation is checked in single-CHP algorithm, which is described in section 4.1.2-Thermal Generation and Storage.

If the availability of CHP generation is confirmed by a household or a third party, the DIGOMIN algorithm runs and the new generations and consumptions are updated. Similar to the first step, Figure 34 shows the procedure for the compensation of deviations by CHP operation.

In the last step, if the CHP operation is restricted to compensate the deviations by local controller, the HP control method is used, described in section 3.3. If the thermal storage is full or local controller does not approve the permission of CHP operation, the HP control approach is used. The cluster agent tries to compensate by applying the step signal (5%, 10%, 15%, and 20%).

The cluster operator tries to compensate by tracking the assigned schedule as close as possible. As shown in Table 4, the signal input of 5% due to lower effect of the output changes has the highest priority and 20% input signal has the lowest priority. If the compensation by HP operation at cluster level is successful, the aggregated agent continues the operation; otherwise, Distribution System Operator (DSO) apply the further measures to supply the excess of the generations. Usually conventional power plants or the other RES supply the excess of generations.

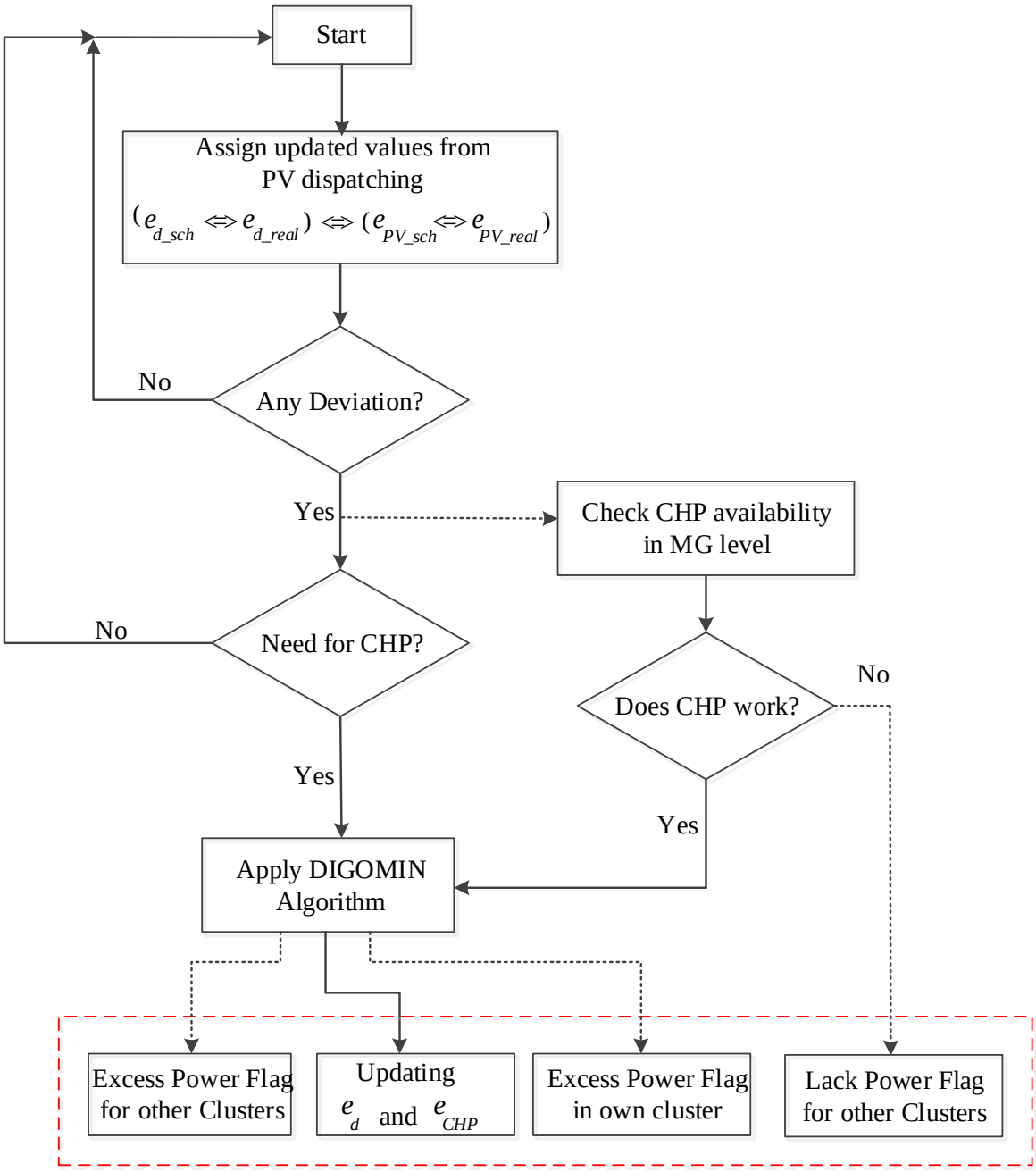

Figure 34: CHP-load balancing algorithm

6. Conclusion

6.1. Case Study and Results

In this part, the described distribution network is simulated in Matlab with the cooperation approach. We considered a time interval of 24 hours, which is divided into 96 time slots of 15 minutes. We assumed that the household power consumption starts at the beginning of the time interval and lasts to the end of the time interval. The network operator confirms the optimal schedule for each household and we randomly create the deviations of the passive loads. Different cases are defined below:

1. Good and variable cloudy weather
2. Ring and radial distribution grid
3. SM/FC prime mover technologies

In the following, a simple scenario for the comparison of different cases is considered. For simplicity, only the ring pattern is studied. First, we assume that the loads are changing randomly among the 19 nodes.

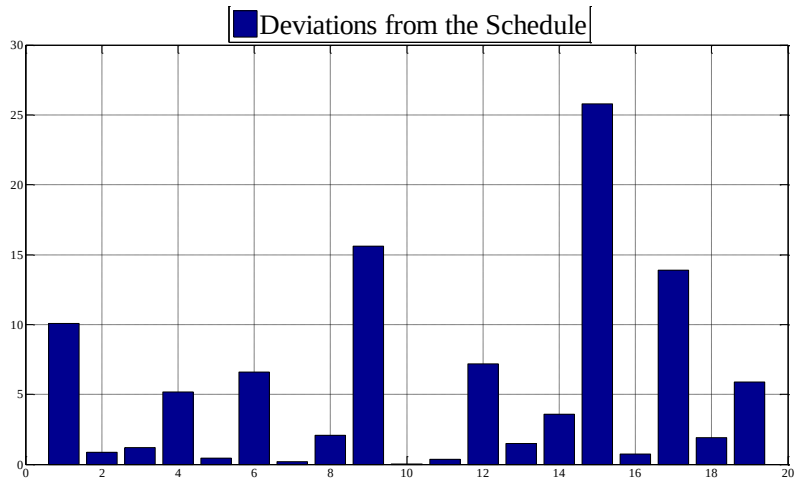

Figure 35: Deviations among the passive loads in certain time interval

These variations take place on the consumers as shown in Figure 35. Based on the priorities, the availability of the PV generations in the conditions of variable cloudy and good weather are shown below:

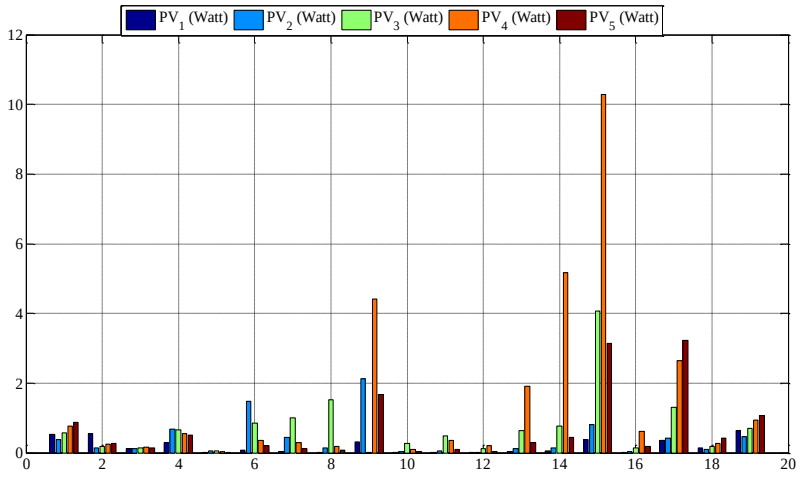

Figure 36: PV Compensation method by optimum dispatching in Variable Cloudy

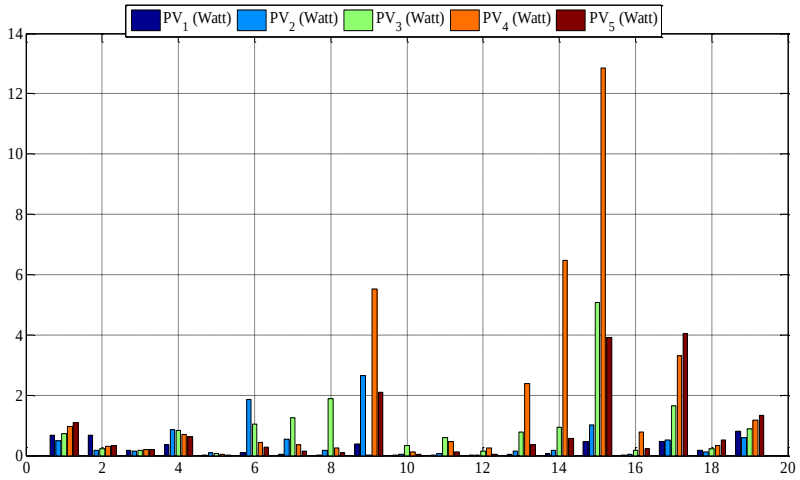

Figure 37: PV Compensation method by optimum dispatching in Good

As shown in Figure 37 and Figure 39, the excess of the PV generations in respect to the expected schedule are dispatched among the deviated loads. The higher generation in the conditions of

good weather in respect to the variable cloudy weather is explained with the higher generation in sunny weather. In the next scenario, the deviations are compensated by two CHPs as in Figure 38.

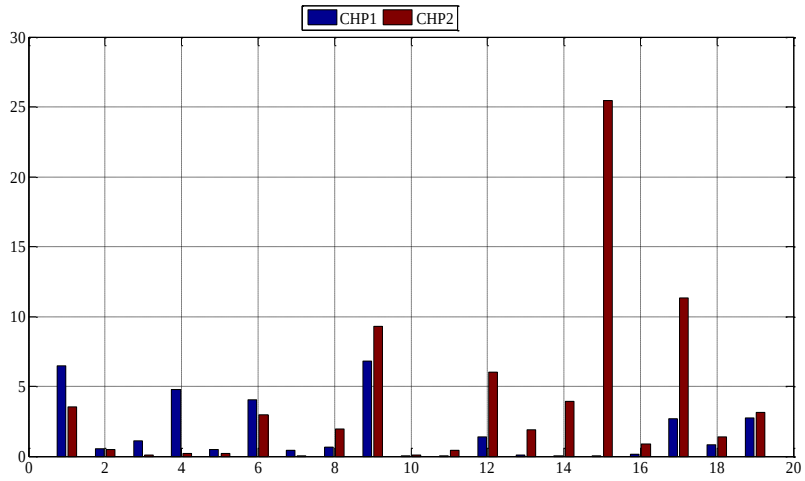

Figure 38: CHP compensation method by optimal dispatching

In the above graph, we assume that the CHPs are located at node 4 and 14. As described in DIGOMIN, the excess of power of the DERs dispatches inversely proportional to the distances.

In this layer if the compensation by the CHPs is not successful, the flexibility of the HP will be checked. According to the transmitted signals, the dynamic behavior of the HP creates the flexibility for network operator for compensate the deviations. According to Table 4, the flexibilities in the higher ratio of the input controlling signals results the higher output and higher flexibilities. The making decision for the network operator to choose one of the options depends on the lack of consumptions. For example, when the storage is almost full and the CHP operation is not possible the network operator can use the flexibility of the HP.

6.2. Summary

In this work, we proposed the methodology for the compensation of the deviated loads by exploitation of PV, HP, and CHP. The method is implemented in Matlab assuming that the consumption and forecast data is available for the agent operator. The network operator compares for each time interval (15 minutes) the current and forecasted consumptions; if the deviations are discovered tries to compensate the unexpected behavior of the passive load according to the DER in the network grid.

The agent operator estimates the PV generations with a KF method in each time interval, according to the weather conditions. One of the options for the network operator in some special cases is to compensate the deviations by excess of PV generations.

The alternative solution is using the CHP system. The CHP according to the thermal storage capacity decides to operate in the grid or not. For SM, the minimum duration of the CHP is assumed 30 minutes and for the FC, 45 minutes.

The last solution is to use the flexibility of the HP as a representative of TCLs. We have defined the dynamic behaviors of the HP in four states. By applying control method, the flexibility of the HP in presence of DR actions was studied. The flexibility of the aggregated model of the HP helps the network operator for compensate the deviations when the thermal storage system is full and CHP operation is restricted.

Finally, a method for dispatching the excess of generation is proposed. This framework helps the network operator to decide how to dispatch the generations among the deviated loads optimally. At the end, a simple case study with PVs and CHP is introduced.

7. Bibliography

[1] M. Houwing And I. Bouwmans, “Agent-Based Modelling of Residential Energy Generation With Micro-CHP.”

[2] S. By, I. Smart, W. Analysis, And B. Y. Zpryme, “Power Systems of The Future : The Case For Energy Storage , Distributed Generation , And Microgrids,” No. November, 2012.

[3] E. Handschin, F. Neise, H. Neumann, And R. Schultz, “Optimal Operation of Dispersed Generation Under Uncertainty Using Mathematical Programming,” No. August, pp. 22–26, 2005.

[4] “Strategic Plan For The Iea Demand-Side,” pp. 1–18, 2012.

[5] V. Hamidi, F. Li, L. Yao, And M. Bazargan, “Domestic Demand Side Management For Increasing The Value of Wind,” pp. 1–10, 2015.

[6] P. Palensky, S. Member, And D. Dietrich, “Demand Side Management : Demand Response, Intelligent Energy Systems, And Smart Loads,” Vol. 7, No. 3, pp. 381–388, 2011.

[7] Y. Guo, A. Zeman, And R. Li, “Utility Simulation Tool For Automated Energy Demand Side Management,” pp. 37–44.

[8] C. Molitor, F. Ponci, A. Monti, D. Cali, And D. Müller, “Consumer Benefits of Electricity-Price-Driven Heat Pump Operation In Future Smart Grids,” pp. 1–4, 2011.

[9] C. Molitor, D. Cali, R. Streblow, F. Ponci, S. Member, D. Müller, And A. Monti, “New Energy Concepts And Related Information Technologies : Dual Demand Side Management,” Innovative Smart Grid Technologies ISGT 2012 IEEE Pes, pp. 1–6, 2012.

[10] J. A. Carr, J. C. Balda, And H. A. Mantooth, “A Survey of Systems To Integrate Distributed Energy Resources And Energy Storage On The Utility Grid,” No. November, 2008.

[11] K. Al Nuaimi, N. Mohamed, M. Al Nuaimi, And J. Al-Jaroodi, “A Survey of Load Balancing In Cloud Computing : Challenges And Algorithms,” pp. 137–142, 2012.

[12] J. H. B. Eng And M. Eng, “The Development , Implementation , And Application of Demand Side Management And Control (DSM + C) Algorithm For Integrating Micro- Generation System Within Built Environment,” No. March, 2009.

[13] W.-L. Hsieh, C.-H. Lin, C.-S. Chen, C. T. Hsu, T.-T. Ku, C.-T. Tsai, And C.-Y. Ho, “Impact of PV Generation To Voltage Variation And Power Losses of Distribution Systems,” 2011 4th International Conference On Electric Utility Deregulation And Restructuring And Power Technologies (Drpt), pp. 1474–1478, Jul. 2011.

[14] A. Trejos, D. Gonzalez, And C. A. Ramos-Paja, “Modeling of Step-Up Grid-Connected Photovoltaic Systems For Control Purposes,” pp. 1900–1926, 2012.

[15] B. Simulation, “Heat Pupm Modelling For Annual Performance , Design And New Technologies Thomas Afjei , Ralf Dott Institute of Energy In Building , University of Applied Sciences Northwestern Switzerland,” pp. 14–16, 2011.

[16] D. Gonzalez, C. Andrés, R. Paja, And A. J. Saavedra, “Modeling And Control of Grid Connected Photovoltaic Systems Modelado Y Control De Sistemas Fotovoltaicos Conectados A La Red Eléctrica,” pp. 145–156, 2012.

[17] M. Houwing, “Smart Heat And Power, Utilizing The Flexibility of Micro Cogeneration,” Technische Universiteit Delft, 2010.

[18] I. Engineers, K. H. Van Dam, M. Houwing, Z. Lukszo, And I. Bouwmans, “Agent-Based Control of Distributed Electricity Generation With Micro Combined Heat And Power,” No. September 2005, 2006.

[19] “The Out Look For Energy: A View To 2040,” 2013.

[20] B. Bletterie, A. Renewable, And E. Resources, “19 Th International Conference On Electricity Distribution Impact of Photovoltaic Generation On Voltage Variations – How Stochastic Is PV ?,” No. 0513, pp. 21–24, 2007.

[21] W. De Soto, S. A. Klein, And W. A. Beckman, “Improvement And Validation of A Model For Photovoltaic Array Performance,” Solar Energy, Vol. 80, No. 1, pp. 78–88, Jan. 2006.

[22] Y. Hosoda And T. Namerikawa, “Short-Term Photovoltaic Prediction By Using H ∞ Filtering And Clustering,” Vol. 0, No. 1, pp. 119–124, 2012.

[23] G. Kerber, “Aufnahmefähigkeit Von Niederspannungsverteilnetzen Für Die Einspeisung Aus Photovoltaikkleinanlagen,” 2011.

[24] R. Rojas, “The Kalman Filter,” pp. 1–7.

[25] T. J. Sturgeon, “Effects of The Crisis On The Automotive Industry In Developing Countries A Global Value Chain Perspective,” No. June, 2010.

[26] R. Halvgaard, N. K. Poulsen, H. Madsen, And J. B. Jørgensen, “Economic Model Predictive Control For Building Climate Control In A Smart Grid,” pp. 1–6.

[27] T. Comfort, Modelling The Dynamics of Domestic Low-Temperature Heat Pump Heating Systems For Improved Performance And Thermal Comfort - A System Approach Dimitra Sakellari. 2005.

[28] J. L. Mathieu, S. Member, S. Koch, And D. S. Callaway, “State Estimation And Control of Electric Loads To Manage Real-Time Energy Imbalance,” Vol. 28, No. 1, pp. 430–440, 2013.

[29] N. Sinitsyn, S. Backhaus, And I. Hiskens, “Modeling And Control of Heat Pumps” 2011.

[30] S. Koch, J. L. Mathieu, And D. S. Callaway, “Modeling And Control of Aggregated Heterogeneous Thermostatically Controlled Loads For Ancillary Services,” 2011.

[31] G. Schlegel, “A Trnsys Model of A Hybrid Lighting System By,” 2003.

[32] “Simulation And Performance Evaluation of Battry Base Stand-Alone Photovoltaic Systems of Malawi,” No. June, 2009.

[33] L. M. Strategies, “Investigation of The Dynamic Behavior of Heat Pumps For The Future Integration In Load Management Strategies” 2011.

[34] F. C. Schweppe, “Physcially Based Modeling of Cold Load Pickup,” No. 9, pp. 4142–4150, 1981.

[35] S. Power, “Statistical Synthesis of Power System Functional Load Model,” 1979.

[36] K. Kalsi, F. Chassin, And D. Chassin, “Aggregated Modeling of Thermostatic Loads In Demand Response,” 2011.

[37] D. P. Chassin And J. C. Fuller, “On The Equilibrium Dynamics of Demand Response In Thermostatic Loads,” 2011 44th Hawaii International Conference On System Sciences, pp. 1–6, Jan. 2011.

[38] D. Baggs And N. Mortensen, “Thermal Mass In Building Design Actions Towards Sustainable Outcomes,” Vol. 1, No. May, 2006.

[39] N. J. Kelly, J. A Clarke, A. Ferguson, And G. Burt, “Developing And Testing A Generic Micro-Combined Heat And Power Model For Simulations of Dwellings And Highly Distributed Power Systems,” Proceedings of The Institution of Mechanical Engineers, Part A: Journal of Power And Energy, Vol. 222, No. 7, pp. 685–695, Nov. 2008.

[40] C. Chemaly, “Micro-CHP In A Residential Area By Modeling The Diffusion of Micro-CHP In A Residential,” 2009.

[41] R. Krawinkler, G. Trnka, And E. Commission, “Micro CHP Systems :,” Vol. 8.

[42] J. W. Turkstra, N. V. N. Gasunie, G. Engineering, H. H. Overdiep, And G. Trade, “The Gasuine Smart Distributed Power Systems Program” 2006.

[43] A. D. Peacock, “Controlling Micro-CHP Systems To Modulate Electrical Load Profiles,” Vol. 32, No. 7, pp. 1093–1103.

[44] M. Houwing, R. R. Negenborn, And B. D. S. Member, “Demand Response With Micro-CHP Systems,” Vol. 19, 2011.

[45] T. A. Faculty And I. P. Fulfillment, “Multi-Agent Based Control of Large-Scale Complex Systems Employing Distributed Dynamic Inference Engine Daili Zhang Multi-Agent Based Control of Large-Scale Complex Systems Employing,” No. May, 2010.

[46] B. N. R. Jennings And S. Bussmann, “Agent-Based Control Systems: Why Are They Suited To Engineering Complex Systems?,” No. June, pp. 61–73, 2003.

[47] I. Engineers, K. H. Van Dam, M. Houwing, Z. Lukszo, And I. Bouwmans, “Agent-Based Control of Distributed Electricity Generation With Micro Combined Heat And Power,” No. September 2005, 2006.

[48] T. A. Faculty And I. P. Fulfillment, “Multi-Agent Based Control of Large-Scale Complex Systems Employing Distributed Dynamic Inference Engine Daili Zhang Multi-Agent Based Control of Large-Scale Complex Systems Employing,” No. May, 2010.

[49] D. H. Scheidt, “Intelligent Agent-Based Control,” pp. 383–395, 2002.

[50] O. Shehory, “Architectural Properties of Multi-Agent Systems,” No. December, 1998.

[51] K. Kok, Z. Derzsi, J. Gordijn, M. Hommelberg, C. Warmer, R. Kamphuis, And H. Akkermans, “Agent-Based Electricity Balancing With Distributed Energy Resources, A Multiperspective Case Study,” Proceedings of The 41st Annual Hawaii International Conference On System Sciences (HICSS 2008), pp. 173–173, Jan. 2008.

[52] C. Lo, S. Member, And N. Ansari, “Decentralized Controls And Communications For Autonomous Distribution Networks In Smart Grid,” Vol. 4, No. 1, pp. 66–77, 2013.

[53] T. Energy And T. Team, “Energy @ Home : A ‘ User-Centric ’ Energy Management System,” pp. 1–7.

[54] D. Livengood And R. Larson, “The Energy Box: Locally Automated Optimal Control of Residential Electricity Usage,” Service Science, Vol. 1, No. 1, pp. 1–16, Mar. 2009.

[55] A. Barbato And G. Carpentieri, “Model And Algorithms For The Real Time Management of Residential Electricity Demand,” 2012 Ieee International Energy Conference And Exhibition (Energycon), pp. 701–706, Sep. 2012.

[56] A. Costabeber, P. Tenti, And P. Mattavelli, “Distributed Cooperative Control of Low-Voltage Residential Microgrids,” 2012 3rd Ieee International Symposium On Power Electronics For Distributed Generation Systems (Pedg), pp. 457–463, Jun. 2012.

[57] T. L. Vandoorn, S. Member, And B. Meersman, “A Control Strategy For Islanded Microgrids With Dc-Link Voltage Control,” Vol. 26, No. 2, pp. 703–713, 2011.

[58] B. A. Vaccaro, M. Popov, D. Villacci, And V. Terzija, “An Integrated Framework For Smart Microgrids Modeling , Communication , And Verification,” 2011.

[59] P. Tenti, A. Costabeber, S. Member, P. Mattavelli, And D. Trombetti, “Distribution Loss Minimization By Token Ring Control of Power Electronic Interfaces In Residential Microgrids,” Vol. 59, No. 10, pp. 3817–3826, 2012.

8. Appendices

Appendix A. Supplementary Details of the PV Model

Temperature	Irradiation	Power
25	1000	131.2333
25	800	100.585
25	600	71.4714
25	400	43.8925
25	200	17.8486

Table 7: The output power of the PV vs. irradiation changes at constant temperature

Temperature	Irradiation	Power
0	1000	146.6701
25	1000	131.2333
50	1000	115.8035
75	1000	100.3807
100	1000	84.9646

Table 8: The output power of the PV vs. temperatures changes at constant irradiation

Temperature	Irradiation	Power
21	900	117.9192
22	920	120.481
23	950	124.5948
24	980	128.7033
25	1000	131.2333

Table 9: The output power of the PV vs. weather condition changes

Appendix B. Supplementary Details of the PV Estimations

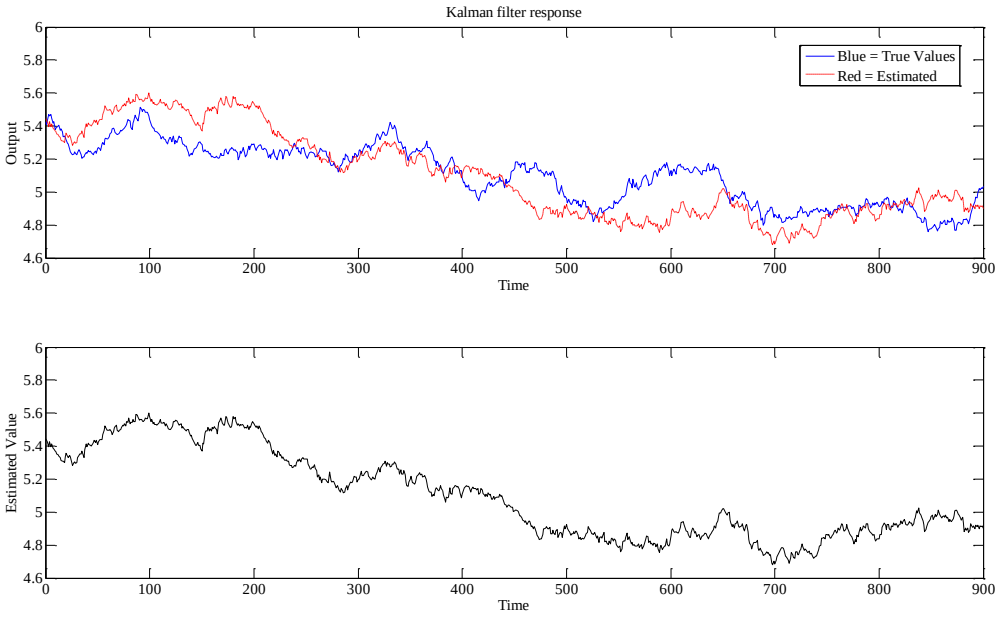

Figure 39: PV generations by applying KF method in Good conditions

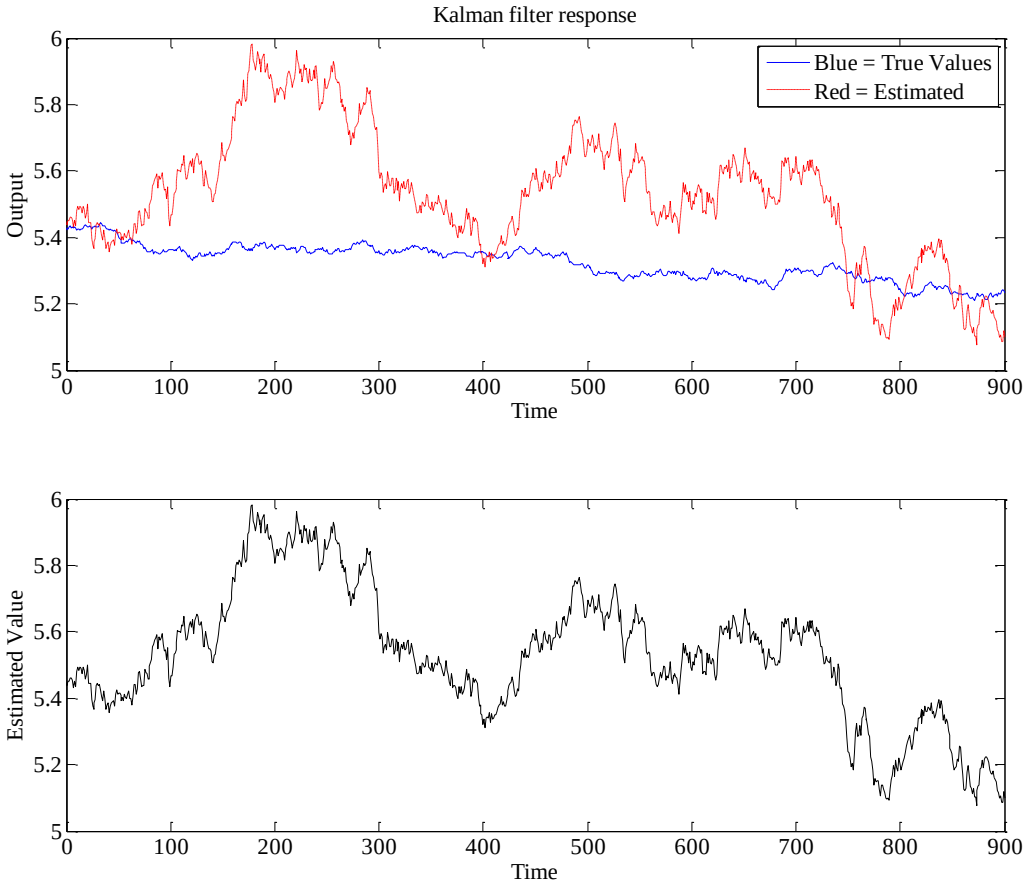

Figure 40: PV generations by applying KF method in Variable Cloudy conditions

Appendix C. Supplementary Details of the HP without DR

The testing scenarios for the HPs in constant and variable duty cycles shown in Figure 41 and Figure 42 respectively. The dashed lines represents the OFF modes and the continuous lines show the ON modes. Figure 41 with variable initial states and constant duty cycle ($\varphi = 40\%$) and Figure 42 for different duty cycles ($\varphi = 30\%, \varphi = 40\%, \varphi = 60\%, \varphi = 70\%$) with identical initial states are depicting the dynamic behavior of the HPs without DR.

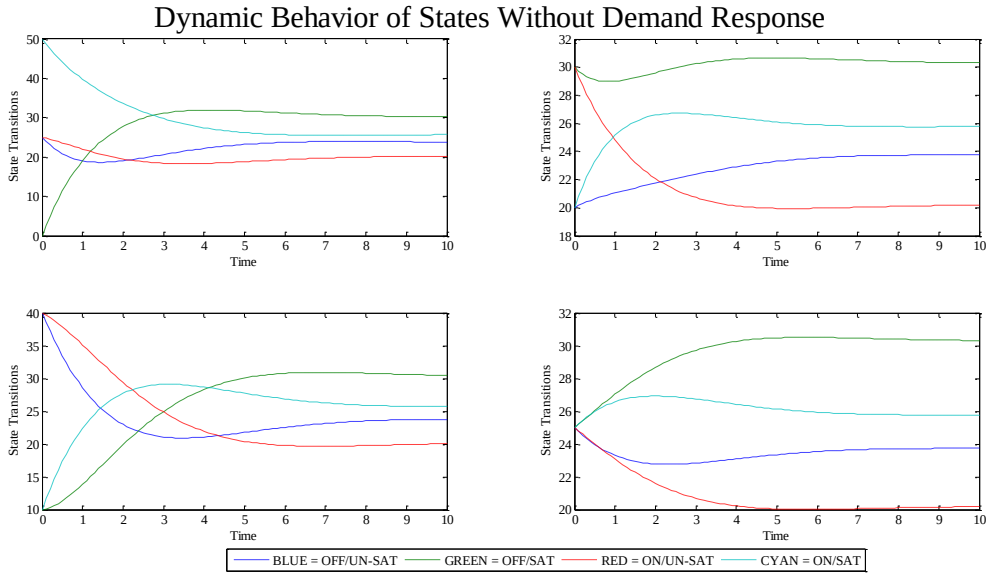

Figure 41: State transitions without demand response by constant duty cycles

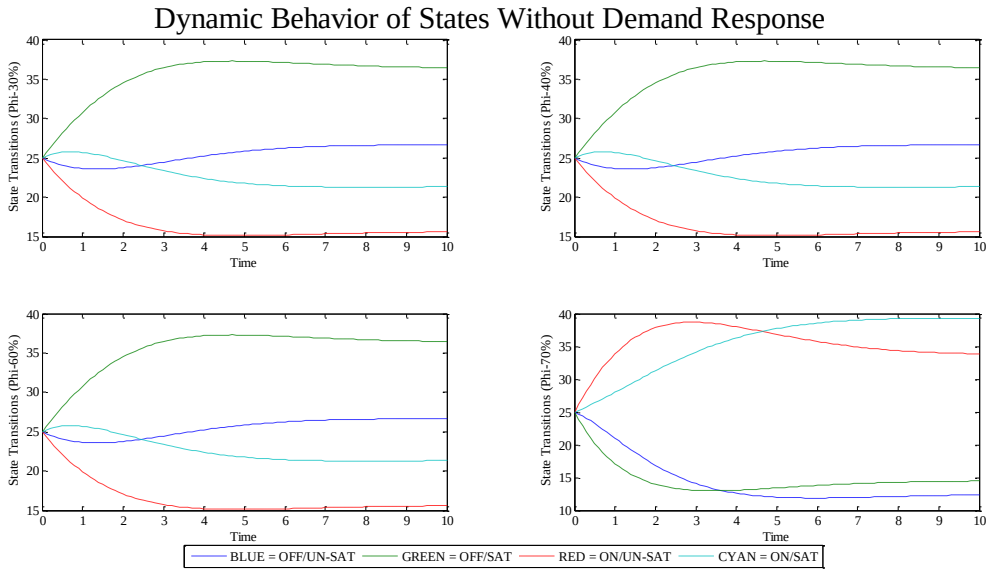

Figure 42: State transitions without demand response for variable duty cycles

Appendix D. Certificates and Publication

This research orally defended for ACS group at E. ON Research Center Institute and approved by committee chair on September 2013. Consequently, the thesis evaluated with an excellent grade at Faculty of Power Engineering of RWTH University in Aachen. Moreover, during my M.Sc. thesis research, I have written and contributed the following scientific paper:

Ivelina Stoyanova, Mehrdad Biglarbegian, and Antonello Monti Cooperative "Energy Management Approach for Short-Term Compensation of Demand and Generation Variations" In Proceedings of the 8th Annual IEEE International Systems Conference, SysCon, Ottawa, Canada, April 2014. (Accepted for publishing)

E.ON Energy Research Center

RWTH

Lehrstuhl für
Automation of Complex Power Systems
Univ.-Prof. A. Monti

E.ON ERC ACS RWTH Aachen Mathieustrasse 10· D-52074 Aachen

Mathieustrasse 10, 52074 Aachen

Telefon +49 241 80-49700
Telefax +49 241 80-49709
amonti@eonerc.rwth-aachen.de
www.eonerc.rwth-aachen.de

18.11.2013

Bescheinigung

Hiermit wird bescheinigt, dass der Student Mehrdad Biglarbegian

(Matr.-Nr.:330 150) seine Masterarbeit mit dem Titel

„Design, Implementation and Evaluation of Methods for Short-term Compensation of Deviations from the Load Schedule for Demand Side Management“

mit der Note 1.3 bestanden hat.

Prof. A. Monti

RWTH Aachen University
E.ON ERC ACS Lehrstuhl für
Automation of Complex Power Systems
Mathieustrasse 10
52074 Aachen
Tel: +49 (0) 241 80 49700
+49 (0) 241 80 49703
Fax: +49 (0) 241 80 49709

FACULTY OF ELECTRICAL ENGINEERING
AND INFORMATION TECHNOLOGY
RWTH AACHEN

TRANSCRIPT OF RECORDS
ACADEMIC YEAR 2012/2013

Sending Institution	POLITECNICO DI MILANO
Faculty/ Department	ENERGY ENGINEERING
Name of student	MEHRDAD BIGLARBEGIAN
Matr.-Nr.:	330150
Receiving Institution	RWTH Aachen University
Faculty/ Department	Fakultät für Elektrotechnik und Informationstechnik
ECTS departmental coordinator	Dr. Hermann Wehr Tel.:+49 241 80 26985 e-mail: wehr@fb6.rwth-aachen.de

Title of the course	**ECTS Credits**	**RWTH Grade**	**ECTS Grade**
Master thesis: Design, implementation and evaluation of methods for short-term compensation of deviations from the load schedule for dual DSM At the Institute of Automation of Complex Power Systems (ACS), RWTH Aachen University Univ.-Prof. Antonello Monti, Ph.D.	30	1.3	A

RWTH grades: 1,0 (best) 1,3 1,7 2,0 2,3 2,7 3,0 3,3 3,7 4,0 5,0 (fail)
ECTS grades: A (best) B C D E Fx (fail) F (fail)

Date 25.11.2013

(Dr. Hermann Wehr, Administrative Director and
ERASMUS/ International Exchange Coordinator)

Cooperative Energy Management Approach for Short-term Compensation of Demand and Generation Variations

Ivelina Stoyanova, Mehrdad Biglarbegian, Antonello Monti
Institute for Automation of Complex Power Systems
E.ON Energy Research Center
Aachen, Germany
istoyanova@eonerc.rwth-aachen.de

***Abstract*— In this work, we introduce the short-term phase of a cooperative energy management algorithm, which exploits the flexibilities arising from the shifted switching of heating systems and charging and discharging of thermal storage. The cooperative approach does not follow any financial gain optimization for individual households but rather targets a solution that is beneficial for all parties involved. We introduce profile deviation categories based on previous studies and define the concept of flexibility provided by the heating systems according to operational boundaries and the capacity of the thermal storage. Within this short-term phase of the energy management algorithm, the switching of the heating systems is coordinated in order to avoid transient effects due to simultaneous switching. Furthermore, occurring deviations from a day-ahead schedule are detected, evaluated and analyzed, and an adequate combination of resources to dispatch is calculated in order to compensate the deviations. The method evaluates short-term weather forecasts and user behavior forecasts, statistical data and signals from the upper grid level. The short-term load compensation is based on local state estimation and includes grid aspects. We present here preliminary results from a case study for a radial grid segment from the model region, in which the combination of dispatch resources is calculated such that their distance from the location of the primary cause of the deviation is minimized.**

Keywords—energy management; demand side management; load variations; flexibility; realtime control

I. INTRODUCTION

InnovationCity Ruhr [1] is a set of projects, which aims to demonstrate the potential of an average city in Germany to integrate renewable energy generation and to achieve significant reduction of its CO2 emissions in a limited period of time. Dual Demand Side Management (2DSM) is a project in InnovationCity Ruhr, which exploits the flexibility arising from the coupling of thermal and electrical supply systems, and storage technologies [2][3]. Major outcomes are: a multi-energy simulation platform and a novel control strategy, based on planning algorithms and short-term control actions.

In this paper, the short-term phase of a cooperative energy management approach is introduced and demonstrated on a sample residential area. In Section II, studies related to the background of the paper and to the modeling and control approaches are presented. Section III describes the system, the assumptions and constraints for the application of the algorithm. The overall energy management approach is presented in Section IV. The short-term compensation algorithm and the results from the case study are introduced in Sections V and VI.

II. RELATED STUDIES

A very mature energy management concept, Triana, is described in [4]. This concept is organized in three phases, prediction, planning and real-time control, similarly to the 2DSM concept. The real-time control is based on an optimization for the balancing of energy flows between pools in the sense of energy sources and sinks. In a further step, an algorithm for model-predictive control is included, in order to reduce negative effects of decisions on later time periods. In Triana, the real-time control operates on the single-device level for every building. Grid aspects are neglected except for the option to account for import and export of energy in the cost functions.

Reference [5] presents a concept for the compensation of solar variations by load-shifting for smart appliances and electric vehicles. The authors suggest the aggregation of negative and positive reserve capacity to smooth PV variations. However, the authors focus on electric vehicles and household devices and do not consider thermal storage.

The approach in [6] suggests the use of aggregated populations of thermostatically controlled loads to manage frequency and energy imbalances. The work is based on state estimation of the electric loads for different levels of real-time communication and available information.

In [7], the authors present an online and offline demand side management optimization models for the control of household appliances and energy storage. Further, a set of heuristics is presented, in order to properly react in real time to unexpected events.

The contribution of this work is to include the consideration of grid aspects and local state estimation in a cooperative setup for the short-term load compensation. The proposed approach

abstracts the control from individual household appliances and focuses on the flexibilities of heating systems and thermal storage, while minimizing the effect on residents' comfort. Furthermore, deviations from the schedule are analyzed individually by every household based on statistics on residents' behavior and forecasts and classified according to the expected duration. The short-term load compensation method is designed as a cooperative approach, which follows global goals beneficial for all participants, rather than the individual goals of the particular household.

III. System Description

A. Framework

For the development of the 2DSM solution, we focused on a scenario with cooperative agents realized within a multi-agent system framework, neglecting financial incentives. The functions and interaction of the agents is described in Section III.B. The energy management approach is based solely on the flexibilities allowed for by the shifted switching of the heating devices and the installed thermal storage. This is explained in more detail in the following.

All households are equipped with a heating system, which can be an electric heater, a heat pump (HP), or a micro Combined Heat and Power (μCHP). Households with a HP or with a μCHP have additionally a thermal storage, which is charged when the heating systems are running. Some households are equipped with photovoltaic modules (PV). Generated PV energy is used to supply the household demand in the first place. In case the generated energy exceeds the household demand, the energy is fed into the grid.

The energy management approach presented here is cooperative and does not follow any financial gain optimization for the individual households. This approach, contrary to the approaches focused on the financial gains of the individual customer, is beneficial for all market participants. On the one hand, customers' monthly expenses can be reduced with increasing amount of installed flexibilities. On the other hand, grid stability is secured and the integration of energy from renewable sources is increased, which saves costs for the grid operator.

For the implementation of the cooperative algorithm, we assume that the customers are willing to switch their heating systems and to feed the surplus of PV generation into the grid as long as their comfort is not penalized. We expect that this scenario is acceptable only if customers do not experience financial disadvantages. An option to solve the financial issues is a flat rate energy tariff similar to internet tariffs, in which the customer pays a basic fee per month, irrespective of their consumption, and accepts requests from the grid operator as far as possible. Such tariff should account for the consumption and offer various basic fees, according to the average power range needed in the household or to the flexibilities the household has actually provided. The tariff could include for example an extra power range for a limited number of hours to cover occasional higher energy consumption, possibly not guaranteed in the peak time. An option for addressing the additional maintenance costs and the reduced life time of the heating systems is that the devices are owned and installed by the energy provider, who keeps the right to switch them when the needs of the household are satisfied, similarly to [9]. However, these billing aspects constitute the viability of the proposed energy management concept in a future energy management structure, which still has to be designed and developed. They are beyond the scope of this work and, therefore, not discussed further.

At the current stage of the project, the 2DSM control algorithm is implemented in a simple hierarchical structure, where the agents aggregate the data received from the lower level, filter relevant data and forward them to the higher level. This structure is not an essential part of the control approach and could be easily replaced by a decentralized structure, in which any of the participants could act as master, for example the building with the highest flexibility in this hour.

B. 2DSM Control Approach

The control approach is organized in two phases. In the first phase, the planning phase, day-ahead schedules are negotiated between the households, represented by Building Agents, and a higher instance, referred to as an Aggregator Agent. The area for which the Aggregator Agent is responsible is referred to as its cluster. In the second phase, the short-term compensation phase, main topic of this paper, the switching of the heating systems is coordinated, and deviations from the schedules are compensated for. Both phases are schematically in Fig. 1 and introduced briefly in the following.

Within the planning phase, which is introduced in the top half of Fig. 1, the Building Agents communicate with an Aggregator Agent, negotiate and agree upon a schedule for the next day in resolution of one hour. The negotiation process is based on forecasts for generation of renewable energy and expected residents' behavior.

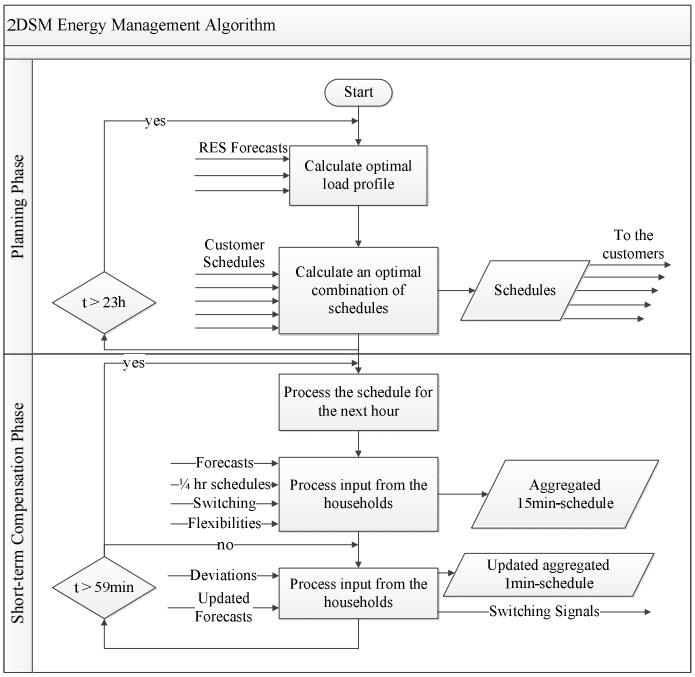

Fig. 1. 2DSM Algorithm: Planning phase and short-term compensation phase

Within the planning phase, which is introduced in the top half of Fig. 1, the Building Agents communicate with an Aggregator Agent, negotiate and agree upon a schedule for the next day in resolution of one hour. The negotiation process is based on forecasts for generation of renewable energy and expected residents' behavior.

Within the short-term phase (described in the bottom part of Fig. 1), occurring deviations from the negotiated schedule are detected and compensated so that the aggregated schedule for the controlled area is kept within certain limits. At the beginning of every hour, in the coordination phase, the schedules for this hour are defined in resolution of 15 minutes by every household. Furthermore, switching of the heating systems is coordinated to avoid transient effects due to simultaneous switching. The compensation algorithm accepts continuously signals for occurring or expected deviations. It is triggered every minute in presence of deviations to find an adequate combination of dispatch resources to compensate the deviations, according to the representation in Fig. 1. The approach is presented in detail in the next chapter.

IV. Short-term Compensation of Deviations

In this section, we introduce deviation categories according to their duration and magnitude and define the concept of provided flexibilities. Deviation categories based on statistical data are useful in systems with limited real-time information and communication, as they can be used to estimate the expected duration and magnitude of the occurring deviations. Even though the deviation categories are based on statistical data, they are grouped by season, week day and time of the day and allow a differentiated view of the detected deviations. For the short-term compensation of deviations, the categories are used to simulate realistic input from a system, for which solely reference values such as the number of residents and socio-economic data are known.

Based on the deviation categories and the flexibility definition, the coordination of switching processes and the compensation of deviations are introduced as key functions of the algorithm.

A. Deviations

According to previous studies, the duration and magnitude of deviations depends on the investigated time interval [10]. They occur more often and with larger magnitudes in the evening hours on weekdays and around noon on weekends. Possibly, this can be explained with the residents' presence and the stochastic nature of consumer behavior. Depending on the region, the demand is subject to specific seasonal variations, such as heating and lights in winter and air conditioning in summer. The study in [11] states an average duration of deviations between 15 and 45 minutes around noon and between 30 and 90 minutes on evenings for weekdays. For weekends, the average duration of deviations is between 15 and 90 minutes around noon and on the early afternoon, and between 15 and 60 minutes in the evening hours. Furthermore, numerous randomly occurring deviations below 5 minutes were detected. In regard to PV variations, studies show that 99% last less than 20 minutes [11] [12].

Based on these considerations, the short-term compensation algorithm is triggered in intervals of one minute in order to update the demand and generation forecasts for the next minute. Deviation signals from the Building Agents are processed and included to the aggregated demand curve for the next m intervals for a deviation with expected duration of m minutes.

B. Flexibilities

In order to maintain awareness of the available flexibilities in the cluster, the heating devices update their flexibility and notify the Aggregator Agent in the coordination phase.

From the operative point of view, the flexibility limits of a heating system are defined by technical constraints and by operational boundaries. This is depicted in Fig. 2 for a µCHP, where the operating area of the heating system is defined by the temperature limits of the thermal storage (on and off areas in the figure). For example, the lower temperature limit is usually around 20°-25°C, and the upper limit could reach 95°C. The operating line expresses the relation of thermal and electrical energy generation for this device, also referred to as its Coefficient of Performance (COP). Depending on the current operating point of the heating system, its flexibility potential is described by the operating line. The operating line is the trajectory of the operating point. The direction in which the operating moves along its trajectory depends on the state of the device (on or off).

Based on these considerations, the flexibility of a household is defined as follows:

$$FL_{rangeN} = \{t_L, t_H \in \mathbb{N}_0 \mid t_L < t_H, 0 \leq t \leq 60\} \quad (1)$$

$$FL_{magnN} = \{P_L, P_H \in \mathbb{R} \mid |P_L| \leq |P_H|, \; 0 \leq |P| \leq P_{HSmax}\} \quad (2)$$

In (1) and (2), FL_{rangeN} and FL_{magnN} are the time and power ranges of the flexibility of household N. P_{HSmax} denotes the upper limit for generation or consumption for the flexible device from operational point of view. t_L and t_H, and P_L and P_H denote the lower and upper limits of the time and the power range of flexibility, respectively. P_H could be less or equal to P_{HSmax}. P_H is equal to P_{HSmax} in case the device offers the flexibility to generate or consume energy in its full capacity.

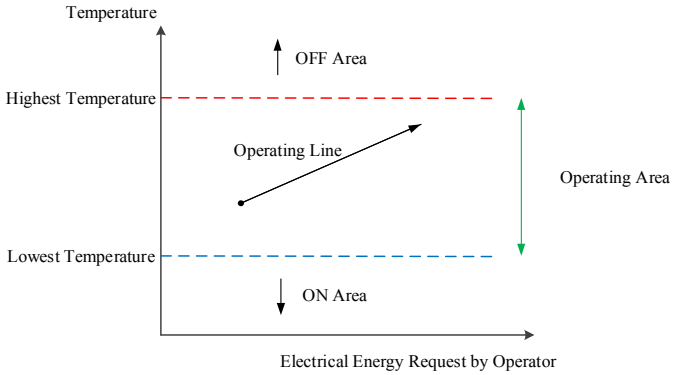

Fig. 2. Flexibility of a µCHP according to the operation area of the device

However, in rare cases it is possible that the device offers flexibility less than P_{HSmax}, for example according to slow-charging settings for electric vehicles.

Positive FL_{magn} denotes the capability of the household to increase its consumption, for example by switching on a HP, between minutes t_L and t_H of the following hour. Power dispatch could be a range ($P_L \neq P_H$, e.g. in case of device capable of modulated operation), or a fixed value ($P_L = P_H$).

C. Coordination

As the negotiated schedules are in a resolution of one hour, the coordination algorithm is executed in the beginning of every hour.

In the coordination phase, the day-ahead forecasts for the generation from regional resources are updated according to short-term weather forecasts. Assuming that the increased share of renewables requires frequent short-term updates at the upper grid level too, the algorithm provides the possibility to distribute the additional energy among the clusters which detected severe deviations. Therefore, in the coordination phase input from the upper grid level is taken into account, so updated generation trends can be adequately addressed and integrated into the grid if possible.

To avoid simultaneous switching and the resulting grid instabilities due to transient switching effects, the switching order of the heating systems is defined in the coordination phase. For the demonstration of 2DSM, a random algorithm inspired by the carrier sense multiple access (CSMA) in communication networks is planned, in order to avoid simultaneous switching of several heating systems. CSMA was developed as an advanced method to overcome the problem of collisions of data frames sent through a communication channel [9]. In CSMA, the sender senses the channel and sends if the channel is idle. If the channel is busy, several strategies are possible:

- 1-persistent CSMA: the sender continuously senses the channel and sends as soon as the channel is idle
- non-persistent CSMA: the sender waits a random amount of time until it senses the channel again
- p-persistent CSMA: the sender waits for the next time slot and sends the frame with (chosen) probability p or waits for the next time slot with probability *q=1-p*

For the proposed energy management approach and the time non-critical applications, such as switching of heating devices and charging of thermal storage, the non-persistent method was chosen. However, in order to implement the method adapted to the coordination of devices, the measuring unit, say, a smart meter, should be able to sense the line and detect if there are transient effects, meaning that another device has just been switched. This solution reduces communication cycles and traffic, but requires units capable of high-resolution measurements. This aspect will be investigated further in future works.

As the performance of the described method cannot be tested in real conditions until the demonstration phase of the project, an alternative method is implemented for the preliminary version of the algorithm. For the validation in simulation, the input of the households which will switch their heating system within the following hour is artificially created by a random generation of a number in the range between 1 and 60, which is considered as their switching time.

Despite its simplicity, the alternative approach is viable as a back-up of the described CSMA-based approach in the demonstration phase. As the transient phase of the considered heating systems is in the range of 1-2 minutes, in systems with limited number of HPs and μCHPs the values should be chosen around the beginning of the 15-minutes intervals, for example ±2 minutes. In case the random switching points interfere, the households receive an alternative switching point such, that there are no two devices switching at the same time.

With a growing number of heating systems in the cluster, the Building Agents will receive more often alternative switching points. As the next project phase foresees their implementation as self-learning systems, they will correct their suggestion range according to the alternative switching points which they received.

D. Compensation Approach

In case of deviations which have to be compensated for, several options are possible for the combination of devices to deliver the dispatch energy. In the following, the principle and the steps are explained schematically for an assumed positive deviation, which means demand higher than expected. The steps are update of the PV generation forecasts, reduction of the consumption by switching off heating systems which consume energy and increased generation by switching on μCHP. The same procedure is followed for negative deviations, with opposite considerations of generation and consumption.

1) Prediction and estimation of PV generation

In the first step, the deviation is compared with the short-term updates for PV generation, assuming that these would increase or decrease the magnitude of the demand deviation.

In order to forecast the PV generation for the next time interval, the parameters initial voltage-current curve, which is calculated analytically, are estimated based on forecast updates, using a linear regression model with a Kalman filter based on [14].

First, the PV characteristics are calculated according to the current weather conditions. We distinguish three weather categories, sunny, cloudy, and variably cloudy as in [12]. The weather categories influence the PV voltage-current curve to a varying degree, according to the different ambient temperature and, therefore, the efficiency factor, and to the generation variability.

For the prediction of the PV generation based on the semi-empirical relations, the current efficiency for the weather conditions and measured values from the last *n* intervals are employed in the regression model in (3).

$$y_k = a_0 + \sum_{i=1}^{n} a_{k-i} y_{k-i} \frac{\eta_k}{\eta_{k-i}} + v_k \qquad (3)$$

In equation (3), y_k is the predicted value for the PV generation for time interval k, based on previous measurements from time intervals from 1 to n, a_0 represents an error model, and η_k and v_k describe the efficiency and the measurement noise at time interval k.

In order to improve the accuracy of the prediction and minimize errors due to unknown modeling parameters in the state-space representation of the system, we implemented a Kalman filter to estimate the state space model and to predict the state transitions in the model based on measurements from the last time intervals.

Based on the PV generation update for the considered interval, the deviation magnitude is updated. In case the PV generation is more than expected, this compensates the higher demand. In case the net total deviation is still outside the predefined limits, the deviation has to be compensated by switching the heating devices. In the following, three possible criteria for the choice of a combination of devices are presented.

2) Compensation of deviations by switching off HPs

Due to technical constraints and issues with the lifetime of the devices, heating systems are blocked for some time after switching. Maximum 3-4 switching actions per hour are technically possible; however, frequent switching should be avoided. If the thermal storage is charged from low to full state of charge (SoC) in one cycle, without interrupting the heating systems, their efficiency and lifetime are increased. Therefore, from the operational point of view, the SoC of the thermal storage is a good criterion for the choice of devices which should be switched. However, this approach is focused on the individual household and is not conform to the cooperative strategy outline. Besides, we expect it to have long-term effects on the energy management algorithm, as it could lead to additional deviations.

Another option is to follow the scheduled SoC in order to keep the demand curve as close as possible to the schedule. This is important for the stability of the overall control algorithm, as the use of flexibilities changes the operation parameters of the addressed households and, therefore, the demand profiles. For example, HPs which are addressed as additional loads, charge their thermal storage during the operation cycle and would be a source of deviations when the storage is fully charged. In this way, the random use of flexibilities increases the level of uncertainty and the probability that approaching the end of the schedule (at 24:00), the allocation of flexibilities does not converge. Therefore, the scheduled SoC is included in the decision process for the addressed devices. This aspect of the short-term compensation algorithm will be a subject of further investigations, as the range of influence of flexibilities use in relation to the installed flexibilities is a part of the validation of the overall algorithm.

The other relevant criterion for the choice of dispatch resources is their physical distance from the cause of the deviation, in order to minimize losses in the system and to avoid congestions. The implemented algorithm searches for the optimal solution for the compensation of the deviation, distributing the excess energy inversely proportional to the distance to the deviation. This strategy is interesting for rural areas due to the long distances between the customers, but also for advanced billing options, such as the option for a group of customers to install a near-district heating system and a combination of generation units and share the energy costs.

For the case study in this paper we assume positive deviation due to higher demand and minimization of losses as a compensation criterion. Therefore, the first compensation step is to switch off energy consuming heating devices, HP, as a zero-loss solution according to [5] and [6].

Reference [5] and [6] describe a coordination method for the control of aggregations of thermostatically controlled loads (TCLs), such as refrigerators and heat pumps. The authors use Markov chain models to describe the temperature evolution of populations of TCLs and a Kalman filtering for state estimation in case of limited information from the system. The authors offer different control options, based on the computation of the probability mass to switch on and off in the next time step due to environment and operational parameters, such as the outside temperature and the operation settings.

Based on the work in [5] and [6], for this work we implemented a simplified state transition model for the HP, as illustrated in Fig. 3, where the possible states are on/off and satisfied/unsatisfied.

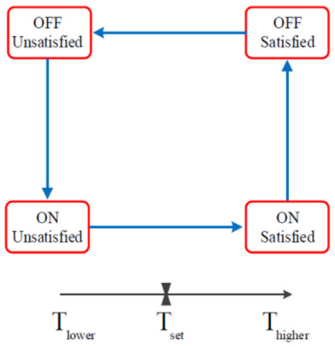

Fig. 3. State transition model for the HP

In order to compensate the occurred deviation, the total amount of power from devices with high probability to be switched in the next time interval is computed; these are the devices in the on and unsatisfied state. According to the deviation magnitude, 5%, 10%, 15% or 20% of the best and good possible combinations of HPs are addressed. In case of a deviation residual, the flexibilities offered by µCHPs are evaluated.

3) Compensation of deviations by switching on µCHPs

The dispatch of generation according to the physical distance to the cause of deviation is based on the principle introduced in [15] and described by equation (4). In (4), loads are indicated with m, and distributed energy sources with n. Accordingly, a deviation at node m due to higher demand is indicated with ΔP_m:

$$P_m^n = \Delta P_m \frac{P_n^{flex}}{d_m^n} \left(\sum_{n=1}^{N} \frac{P_n^{flex}}{d_m^n} \right)^{-1} \quad (4)$$

In (4), the contribution P_m^n of node n is calculated according to its distance to the deviation d_m^n and its flexibility P_n^{flex}. The consideration of the distance to the deviation for all distributed energy sources introduces an optimal dispatch solution for the compensation of the deviation.

In the discussed case of higher demand than scheduled, the procedure is applied to the µCHPs that offered flexibility for the considered time interval. In the last step of the compensation procedure, deviation residuals are offered to neighborhood areas or announced to the higher grid level.

Further development of the algorithm will include the consideration of several criteria; for which both steps will be combined and weighted.

V. CASE STUDY

In this section, preliminary results from a case study are presented for a radial grid segment from the model region. In order to illustrate the performance of the presented algorithm, two scenarios are studied for a realistic deviation vector, according to the level of penetration of flexible heating systems in the residential area. The tests are focused on the potential for the compensation of deviations at local level. In particular, we study the reduction of losses with the implemented algorithm which was described in the previous section. The level of penetration of flexible heating systems is modeled by simulating different combinations of HPs and µCHPs in the residential area.

The tests were done on a radial grid segment in a residential area, as illustrated in Fig. 4. The test scenario maps an existing area within the model region. The grid characteristics, the modeled buildings and the geographical relations reflect the real circumstances in the area.

The grid segment consists of 19 nodes, each corresponding to a building. Many buildings are apartment buildings with up to eight households. There are 62 households in total, with one to five residents. We used the average values calculated in the study on load variations in residential areas in [11], and scaled them according to the characteristics of the test scenario for the time 11:00-12:00 on a Sunday in winter. The deviation categories scaled for a household of four residents are illustrated in TABLE I.

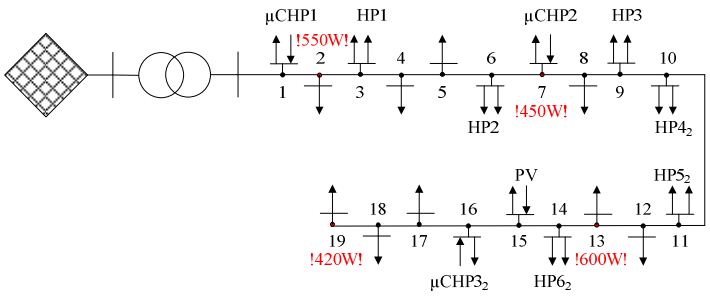

Fig. 4. Grid segment of the case study

TABLE I. DEVIATION CATEGORIES FOR A HOUSEHOLD OF FOUR PEOPLE

	Weekday			
	Summer		***Winter***	
Time slot	**Magnitude**	**Duration**	**Magnitude**	**Duration**
07:30-09:30	Up to 125W	Up to 20min	Up to 175W	Up to 15min
11:30-14:30	Up to 250W	15-45 min	Up to 300W	15-35 min
17:30-22:00	Up to 425W	45-90 min	Up to 425W	30-70 min
	Saturday			
	Summer		***Winter***	
Time slot	***Magnitude***	***Duration***	***Magnitude***	***Duration***
10:00-12:00	Up to 200W	Up to 45min	Up to 100W	Up to 20min
12:30-16:00	Up to 550W	20-60 min	Up to 500W	20-60 min
19:30-22:00	Up to 175W	Up to 20min	Up to 500W	15-70 min
	Sunday			
	Summer		***Winter***	
Time slot	***Magnitude***	***Duration***	***Magnitude***	***Duration***
9:00-15:00	Up to 500W	30-90 min	Up to 425W	15-90 min
18:00-22:30	Up to 375W	15-70 min	Up to 325W	15-60 min

According to the frequency of occurrence of deviations in [11], we implemented following four deviations:

- Node 19 (a 3-person household): deviation with a magnitude of 420 W and a duration of 45 minutes
- Node 13 (a 5-person household): deviation with a magnitude of 600 W and a duration of 40 minutes
- Node 2 (a 5-person household): deviation with a magnitude of 550 W and a duration of 30 minutes
- Node 7 (a 4-person household): deviation with a magnitude of 450 W and a duration of 35 minutes.

Both test scenarios are illustrated in Fig. 4, where the flexible resources (HPs and µCHPs) are illustrated as additional load or generation at the corresponding nodes. The additional resources considered only for the advanced test scenario are indexed with "$_2$". All households with flexible heating devices have thermal storage, which allows them to generate (µCHPs) or consume energy (HPs) when addressed with a corresponding request.

A. Basic Scenario

In the basic scenario flexible heating systems are modeled at node 3, 16 and 17 (HP1, HP2, HP3), and at nodes 1 and 7 (µCHP1 and µCHP2). Their scheduled operation modes, SoC and flexibility for the time 10:00-13:00 are listed in TABLE II.

The scheduled operation mode, listed as "Schedule" in Table II, is 0 for devices, which are off within this hour, 1 for devices running and consuming electrical energy, and -1 for devices running and generating energy. As described in Section IV.B, positive flexibility power range denotes the possibility of

the household to increase its energy demand. For example, according to the schedule for the time slot 11:00-12:00, the thermal storage of HP1 is charged to 33% at the beginning of the time slot. HP1is scheduled to be running between 11:00 and 12:00. It offers flexibility to reduce its consumption by 400 W ($FL_{magn} = -0.4$ kW) at any time ($FL_{range} = \{0, 60\}$min) if necessary. Further negative flexibilities are provided by µCHP1 and µCHP2, which could increase their generation by 370 W and 540 W, respectively.

TABLE II. SCHEDULES AND FLEXIBILITIES FOR THE RESOURCE IN THE BASIC SCENARIO

Time Slot	Parameters	HP1	HP2	HP3	µCHP1	µCHP2
10:00 - 11:00	***Schedule***	1	0	0	-1	-1
	SoC	37%	35%	70%	46%	55%
	FL_{range} ***[min]***	{0, 60}	{0, 60}	{0, 60}	{0, 60}	{0, 60}
	FL_{magn} ***[kW]***	{− 0.4}	{1.0,5.0}	{1.0,3.0}	{−0.37}	{−0.54}
11:00 - 12:00	***Schedule***	1	1	0	-1	-1
	SoC	43%	30%	69%	53%	64%
	FL_{range} ***[min]***	{0, 60}	{0, 60}	{0, 60}	{0, 60}	{0, 60}
	FL_{magn} ***[kW]***	{−0.4}	{0}	{1.0,3.0}	{−0.37}	{−0.54}
12:00 - 13:00	***Schedule***	1	1	0	-1	-1
	SoC	49%	41%	68%	60%	73%
	FL_{range} ***[min]***	{0, 60}	{0, 60}	{0, 60}	{0, 60}	{0, 60}
	FL_{magn} ***[kW]***	{− 0.4}	{0}	{1.0,3.0}	{−0.37}	{−0.54}

1) *Coordination*

HP2 is scheduled to be off in the time slot 10:00-11:00, and to be running in the next time slot due to the low SoC of the thermal storage (30%). The device generates a random a number for its preferred starting time (minute 42) and sends a signal to the Aggregator Agent.

The short-term PV forecast updates indicate expected generation increase by 400 W.

2) *Deviation processing and compensation*

The deviations described above are illustrated in Fig. 5. The increased PV generation reduces the net total deviation to 1620 W.

The distance between the µCHPs and the loads are illustrated in Fig. 6. According to the distance to the deviations and equation (4), Fig. 6 shows the optimal solution for loss-efficient energy dispatch from both µCHPs among the deviations. The µCHP1 would be the most efficient option to compensate the deviation at node 2 due to the very short distance of 5m between the nodes. The adequacy of µCHP1 for the compensation of the other deviations decreases with the distance to nodes 7, 13 and 19.

This conclusion is confirmed by the compensation adequacy of µCHP2 at node 7. As there is a detected deviation at the same node, the most efficient solution is to assign the same resource for its compensation.

By switching HP1 and both µCHPs, the initial deviation of 1620 W was reduced to 310 W. In this case, the deviation signal would be announced to the upper grid level or communicated with neighbor clusters as described in Section IV.

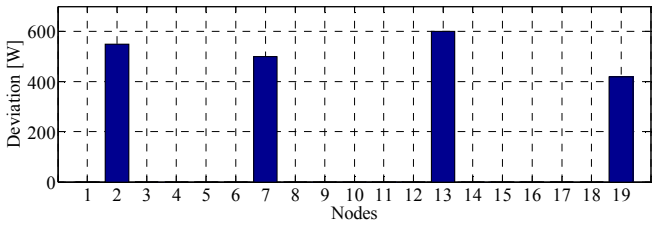

Fig. 5. Deviations in the time 11:15-11:50

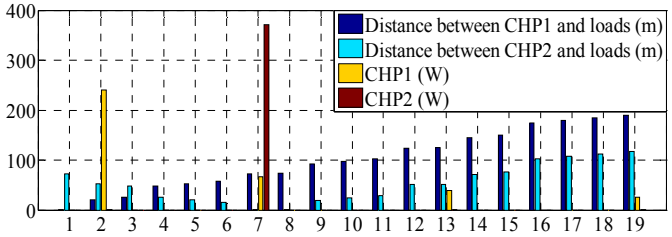

Fig. 6. Distance to the loads and corresponding adequacy for compensation of the deviations in the basic scenario

B. *Advanced Scenario*

For the advanced scenario, further 3 HPs (HP4, HP5 and HP6 at nodes 10, 11 and 14), and µCHP3 at node 16 were included. The schedules and flexibilities for the resources introduced in the basic scenario are considered the same. The parameters of the additional resources are listed in TABLE III.

TABLE III. SCHEDULES AND FLEXIBILITIES FOR THE RESOURCES ADDED FOR THE ADVANCED SCENARIO

Time Slot	Parameters	HP4	HP5	HP6	µCHP3
10:00 - 11:00	***Schedule***	0	1	0	-1
	SoC	62%	44%	70%	46%
	FL_{range} ***[min]***	{0, 60}	{0, 60}	{0, 60}	{0, 60}
	FL_{magn} ***[kW]***	{1.2, 3.6}	{−0.3}	{0}	{−0.54}
11:00 - 12:00	***Schedule***	0	1	1	-1
	SoC	61%	47%	68%	53%
	FL_{range} ***[min]***	{0, 60}	{0, 60}	{0, 60}	{0, 60}
	FL_{magn} ***[kW]***	{1.2, 3.6}	{−0.3}	{0}	{−0.54}
12:00 - 13:00	***Schedule***	0	1	1	-1
	SoC	60%	50%	72%	60%
	FL_{range} ***[min]***	{0, 60}	{0, 60}	{0, 60}	{0, 60}

	FL_{magn} **[kW]**	{1.2, 3.6}	{−0.3}	{0}	{−0.54}

1) Coordination

Within the coordination phase, the Aggregator Agent receives the signal from HP2 as described in the basic scenario, and a signal from HP6 that it will switch on at minute 21 of the current hour. As the switching times do not interfere, no further actions are required from the Aggregator Agent. The short-term PV updates indicate generation increase by 400 W.

2) *Deviation processing and compensation*

The deviation vector is the same as for the basic scenario. The distance from the µCHPs to the nodes is illustrated in Fig. 7. Again, µCHP1 is the most efficient option to compensate the deviation at node 2. µCHP2 is the optimal compensation resource for the deviation at the same node. µCHP3 at node 16 should be addressed as first resource for the compensation at node 19 and, to a limited extent, for the deviation at node 13.

The three µCHPs offer flexibility potential of ca. 1450 W, which compensates completely the deviation residual of 920 W after the PV update and after switching off HP1 and HP5. According to Fig. 7, the most adequate combination of resources for the deviation compensation with minimal losses is µCHP2 and µCHP3. This assumption is validated by simulation of the optimal combination and of random switching combinations, which are µCHP1 and µCHP2 or µCHP3. The simulation results are listed in TABLE IV.

We assume that the deviation residuals of 10 W and -160 W are both within the preset limits. The grid losses of 752 W and 750 W for random switching are higher than the calculated losses of 736 W for the optimal resource combination.

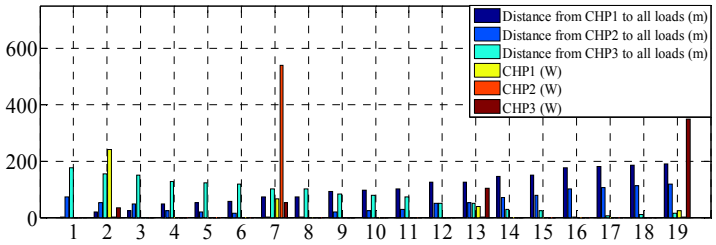

Fig. 7. Distance to the loads and corresponding adequacy for compensation of the deviations in the advanced scenario

TABLE IV. NETWORK LOSSES AND DEVIATION RESIDUAL FOR THE COMBINATIONS OF RESOURCES

Combination	Network Losses	Deviation Residual
µCHP1 and µCHP2	752 W; 536 Var	10 W
µCHP1 and µCHP3	750 W; 541 Var	10 W
µCHP2 and µCHP3	738 W; 536 Var	-160 W

VI. CONCLUSIONS

In this work, an approach for the short-term compensation of deviations is presented as a part of a two-phase energy management algorithm. We define the concept of provided flexibilities and introduce statistical deviation categories.

The short-term compensation approach starts with the coordination of heating devices in order to avoid transient effects due to simultaneous switching. The compensation of deviations can follow different priorities. Here we calculate the combination of dispatch resources such that the physical distance to the deviation cause and, therefore, the losses are minimal.

We demonstrate the presented algorithm on a grid segment with 19 nodes and 62 households which reflects the real conditions in an area in the model region of the project. The generation of the deviation signal is based on statistical studies and shows the applicability of statistical load-deviation data in systems with minimal real-time information exchange.

The simulation confirms the applicability of the compensation approach for realistic conditions. The decreased grid losses for the optimal combination of dispatch resources compared to random switching confirm the adequacy of the implemented loss minimization algorithm.

REFERENCES

[1] InnovationCity Ruhr [Online]. Available: http://www.bottrop.de/microsite/ic/, last visited: Sept. 2013

[2] C. Molitor et al., "New energy concepts and related information technologies: Dual Demand Side Management," in *Proc. Innovative Smart Grid Technologies (ISGT), 2012 IEEE PES* , pp.1,6, 2012

[3] I. Stoyanova et al., "Challenges in modeling a multi-energy system at city quarter level," in *Proc. COMPENG 2012, IEEE Workshop on Complexity in Engineering*.

[4] A. Molderink, "On the three-step control methodology for Smart Grids," PhD thesis, University of Twente, 2011. ISBN 978-90-365-3170-2

[5] J.L. Mathieu, S. Koch, D.S. Callaway, "State Estimation and Control of Electric Loads to manage real-time energy imbalance," *Power Systems, 2013 IEEE Transactions on* , vol. 28, no. 1, pp.430-440, Feb. 2013

[6] Mathieu, J.L.; Callaway, D.S., "State Estimation and Control of Heterogeneous Thermostatically Controlled Loads for Load Following," *System Science (HICSS), 2012 45th Hawaii International Conference on* , vol., no., pp.2002,2011, 4-7 Jan. 2012

[7] A. Schuelke, K. Erickson, "Serving solar variations with consumption control of smart appliances and electric vehicles," *Innovative Smart Grid Technologies (ISGT Europe), 2011 2nd IEEE PES International Conference and Exhibition on* , vol., no., pp.1,8, 5-7 Dec. 2011

[8] A Barbato, G. Carpentieri, "Model and algorithms for the real time management of residential electricity demand," in *Proc. IEEE International Conference and Exhibition, ENERGYCON '12*, 2012.

[9] Lichtblick – die Zukunft der Energie [Online]. Available: http://www.lichtblick.de/, last visited: Sept. 2013

[10] IEEE 802.15.4-2006, Chapter 7.5.1.4 CSMA-CA algorithm.

[11] I. Stoyanova, M. Marin, A. Monti, "Characterization of load profile deviations for residential buildings," in *Proc. Innovative Smart Grid Technologies (ISGT), 2013 IEEE PES*, 2013

[12] G. Kerber, "Aufnahmefähigkeit von Niederspannungsverteilnetzen für die Einspeisung aus Photovoltaikanlagen," Ph.D. dissertation, Dept. Of El. Eng. and Inf. Techn., Technische Universität München, 2011

[13] W. Jewell, "Issues in utility-interactive photovoltaic generation", IEEE Power Engineering Review, April 1994

[14] Y. Hosoda, T. Namerikawa, "Short-Term Photovoltaic Prediction By Using H ∞ Filtering And Clustering,", *SICE Annual Conference (SICE), 2012 Proceedings of* , vol., no., pp.119,124, 20-23 Aug. 2012.

[15] A. Costabeber, P. Tenti, and P. Mattavelli, "Distributed cooperative control of low-voltage residential microgrids," 2012 3rd IEEE International Symposium on Power Electronics for Distributed Generation Systems (PEDG), pp. 457–463, Jun. 2012.